

Photosensitiser-gold nanoparticle conjugates for photodynamic therapy of cancer

Paula García Calavia^a, Gordon Bruce^b, Lluís Pérez-García^b and David A. Russell^{a*}

^a School of Chemistry, University of East Anglia, Norwich Research Park, Norwich, NR4 7TJ UK

^b School of Pharmacy, University of Nottingham, University Park, Nottingham, NG7 2RD UK

Abstract

Gold nanoparticles (AuNPs) have been extensively studied within biomedicine due to their biocompatibility and low toxicity. In particular, AuNPs have been widely used to deliver photosensitiser agents for photodynamic therapy (PDT) of cancer. Here we review the state-of-the-art for the functionalisation of the gold nanoparticle surface with both photosensitisers and targeting ligands for the active targeting of cancer cell surface receptors. From the initial use of the AuNPs as a simple carrier of the photosensitiser for PDT, the field has significantly advanced to include: The use of PEGylated modification to provide aqueous compatibility and stealth properties for *in vivo* use; Gold metal-surface enhanced singlet oxygen generation; Functionalisation of the AuNP surface with biological ligands to specifically target over-expressed receptors on the surface of cancer cells and; The creation of nanorods and nanostars to enable combined PDT and photothermal therapies. These versatile AuNPs have significantly enhanced the efficacy of traditional photosensitisers for both *in vitro* and *in vivo* cancer therapy. From this review it is apparent that AuNPs have an important future in the treatment of cancer.

Introduction

The use of gold nanoparticles (AuNPs) in biomedicine has been widely studied due to their exceptional biocompatibility and low toxicity.^{1–3} In particular, AuNPs have been found to be ideal delivery agents for photosensitisers in photodynamic cancer therapy (PDT). The combination of photosensitisers with gold nanoparticles has several advantages, including the enhancement in the production of singlet oxygen and other reactive oxygen species, the possibility to disperse hydrophobic photosensitisers in aqueous solutions, and the ability to conjugate biological ligands to the photosensitiser-AuNPs for active targeted PDT.¹ The use of gold nanoparticles for PDT is not limited to spherical nanoparticles. Other gold nanomaterials, including nanorods, nanostars and nanoclusters have also been reported as delivery agents for PDT.¹ Interestingly, the use of other gold nanomaterials and shapes, especially gold nanorods, opens the possibility to combine PDT with other therapies such as photothermal cancer therapy (PTT).⁴

Photosensitisers can be conjugated to the AuNPs through different approaches based on self-assembly. The use of these approaches, including covalent binding and electrostatic interactions, for the functionalisation of gold nanoparticles with photosensitisers will be described in this review. Furthermore, the use of active targeting for selective internalisation of the photosensitisers by specific cancer cells will also be reviewed.

Self-assembly *via* a sulfur-gold bond

The conjugation of photosensitisers to AuNPs *via* self-assembly was first reported by Russell and co-workers.⁵ In this work, a three-component system was synthesised based on a novel substituted zinc phthalocyanine with a C₁₁ mercaptoalkyl tether (C11Pc) self-assembled to the surface of AuNPs (2-4 nm in diameter) in the presence of the phase transfer reagent tetraoctylammonium bromide (TOAB) (**Figure 1a**). The interaction between C11Pc and TOAB in the functionalised AuNPs (C11PcAuNPs) led to a considerable increase in singlet oxygen quantum yield, from ϕ_{Δ} =0.45 to ϕ_{Δ} =0.65, as compared to the free C11Pc in solution. Additionally, the presence of TOAB was beneficial for the systemic administration of the photosensitiser for PDT since it allowed the solubilisation of C11Pc in polar solvents.⁵ The three-component system was subsequently tested *in vitro* using HeLa cervical cancer cell line.⁶ Following a 4-hour incubation, the C11Pc-functionalised AuNPs were successfully internalised by the HeLa cells, as shown in **Figure 1b**. Irradiation with a 690 nm diode laser for 20 minutes induced a photodynamic efficacy leading to 57 % cell death, a significant improvement from the 26 % cell death achieved when the free C11Pc was incubated with the cells.⁶ The PDT efficacy of these C11PcAuNPs were then examined *in vivo*, as reported by Camerin *et al.*⁷ C57 mice subcutaneously implanted with amelanotic melanoma were treated with the C11PcAuNPs, dispersed in a Cremophor EL emulsion, *via* intravenous injection. The C11PcAuNPs largely accumulated within the tumour tissue, in significantly higher concentrations than the free C11Pc, and irradiation of the mice 3 h after injection successfully inhibited tumour growth leading to the animals staying tumour-free for *ca.* 6 days. The three-component system therefore showed significant advantages with respect to the free photosensitiser. To enhance the PDT efficacy of the C11PcAuNPs, a larger concentration of the nanoparticle conjugates was required. However, this required a higher concentration of Cremophor emulsion which would be toxic *in vivo*.⁷

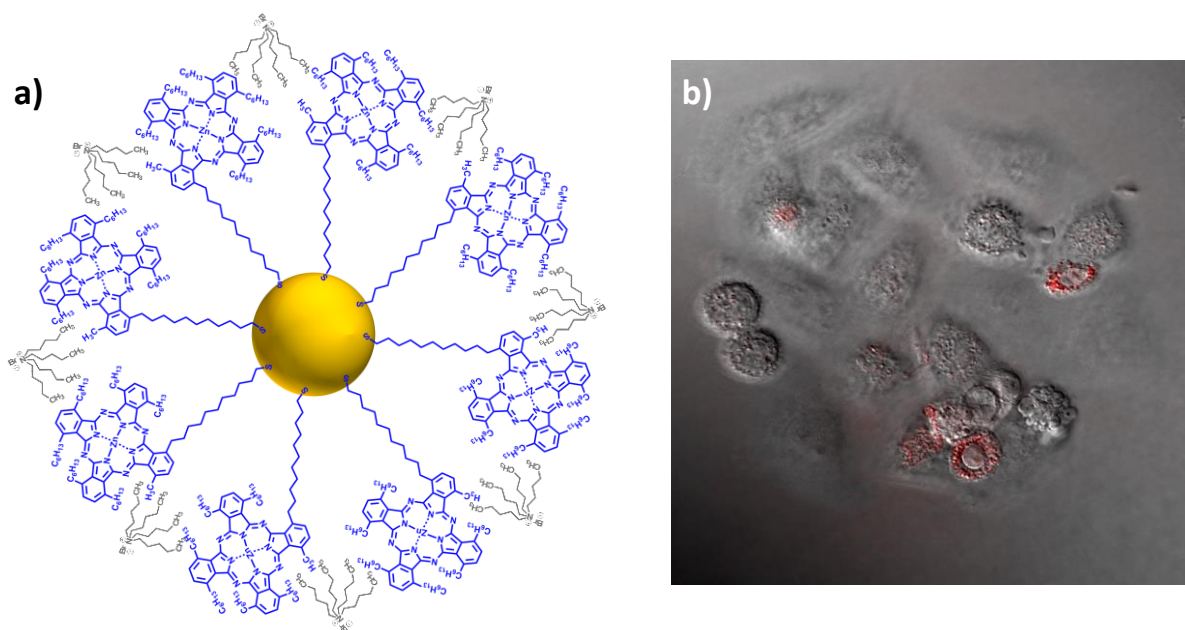


Figure 1. (a) Schematic representation of the synthesised C11PcAuNPs with the phase transfer reagent TOAB. **(b)** Combined confocal fluorescence and DIC images of HeLa cells following incubation with phthalocyanine-nanoparticle conjugates. The presence of the nanoparticle conjugates within the HeLa cells can be readily seen from the fluorescence emission (red) following excitation at 633 nm. Images reproduced from Wieder *et al.*⁶ with permission from the European Society for Photobiology, the European Photochemistry Association and the Royal Society of Chemistry.

The retention of the photosensitiser in the serum, which is essential for PDT, can be enhanced by addition of polyethylene glycol (PEG).⁸ PEG is not only approved for human intravenous application but it also has a high resistance to protein adsorption, thus having the potential to avoid opsonisation by the reticuloendothelial system (RES).¹ Russell and co-workers synthesised a novel nanoparticle system consisting of AuNPs functionalised with a mixed monolayer of PEG and C11Pc (C11Pc-PEG-AuNPs) (**Figure 2a**).⁹ The presence of PEG allowed for the solubilisation of the C11Pc-PEG-AuNPs in aqueous solutions. A further benefit of using PEG is the ability to conjugate the molecule to other biological ligands that can be used for targeted PDT, which will be discussed later. The water-dispersible C11Pc-PEG-AuNPs were used *in vivo* to treat C57/BL6 mice implanted with subcutaneous B78H1 amelanotic melanoma. The C11Pc-PEG-AuNPs were found in the serum in high quantities and were subsequently activated by light irradiation either 3 h or 24 h following injection. As shown in the Kaplan-Meier survival plot in **Figure 2b**, irradiation at 3 h induced the best results, leading to complete survival and no tumour-regrowth in 40 % of the treated mice. The tumour cell death was found to occur primarily due to vascular PDT damage. Furthermore, the authors

found that, after initial accumulation of the C11Pc-PEG-AuNPs in the serum, the nanoparticles moved towards the liver and spleen *ca.* 1 week after injection, leading to excretion *via* the bile-gut pathway.⁹

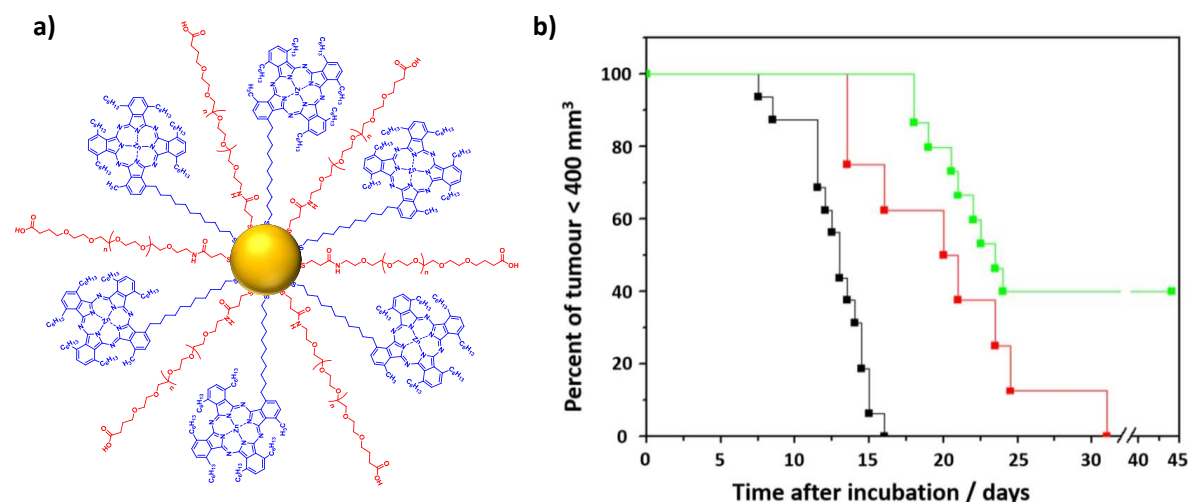


Figure 2. (a) Schematic representation of the synthesised C11Pc-PEG-AuNPs. **(b)** A Kaplan-Meier survival plot highlighting the responses of amelanotic melanoma following photodynamic therapy with the C11Pc-PEG-AuNPs. Black squares: control group (no conjugates injected), $n = 15$; red squares: mice treated 24 hours after injection of conjugates, $n = 8$; green squares: mice treated 3 hours after injection of conjugates, $n = 15$. Image reproduced from Camerin *et al.*⁹ with permission from the European Society for Photobiology, the European Photochemistry Association and the Royal Society of Chemistry.

As shown by Camerin *et al.*,⁹ the pegylated C11PcAuNPs proved to be ideal for *in vivo* PDT, leading to high photodynamic efficiency and tumour destruction. The zinc phthalocyanine photosensitiser chosen for these studies, C11Pc, was designed with a 11-atom carbon chain that connects the macrocycle of the phthalocyanine to the disulfide bond, which would allow for self-assembly to the surface of the AuNPs. The long carbon chain was chosen to avoid quenching of the fluorescence of the phthalocyanine due to interaction with the metallic core of the AuNPs. However, metal-enhanced fluorescence (MEF), by which the fluorescence of fluorophores placed near the surface of metallic nanoparticles can be enhanced, is gaining interest for PDT.^{10,11} MEF has been shown to be related to metal-enhanced singlet oxygen production (ME^1O_2), which would thus lead to an enhanced PDT effect.¹² Both MEF and ME^1O_2 are distance-dependent; fluorophores placed on or close to the metallic core of the nanoparticles can lead to fluorescence quenching but fluorophores placed between *ca.* 5–30 nm from the metal surface can lead to MEF.^{12,13} Russell and co-workers compared the

efficacy of the C11Pc photosensitiser to another substituted zinc phthalocyanine with a C₃ mercaptoalkyl tether (C3Pc).¹⁰ The core of the phthalocyanines was the same for C11Pc and C3Pc, the only difference between the two was the length of the carbon chain that connects the macrocycle to the AuNPs (**Figure 3a**). The authors synthesised AuNPs with a mixed monolayer of PEG and either C11Pc or C3Pc, yielding *ca.* 4 nm water-stable C11Pc-PEG-AuNPs and C3Pc-PEG-AuNPs. While the C11Pc photosensitiser had a higher fluorescence in solution, once conjugated with the AuNPs the C3Pc photosensitiser was found to be more fluorescent due to MEF. The increase in fluorescence for the C3Pc-PEG-AuNPs was correlated with an increased production of singlet oxygen (¹O₂). Both types of nanoparticles were tested *in vitro* with SK-BR-3 human breast adenocarcinoma cells. Internalisation of the nanoparticles was efficient for both but, upon irradiation at 633 nm, the C3Pc-PEG-AuNPs induced a far greater PDT effect (**Figure 3c**) than the C11Pc-PEG-AuNPs (**Figure 3b**), as a consequence of the enhanced production of ¹O₂. Cell viability was further confirmed using a CellTiter-Blue® cell viability assay, which showed that the PDT with the C11Pc-PEG-AuNPs (**Figure 3d**) induced negligible cell death while PDT with the C3Pc-PEG-AuNPs (**Figure 3e**) produced 85 % cell death with low C3Pc concentrations of 0.23 μM.¹⁰ This study highlights the importance of MEF for photodynamic therapy. Engineering the distance between the photosensitisers and the AuNPs can have a significant effect in PDT, leading to higher levels of cell death at lower concentrations of the drug.

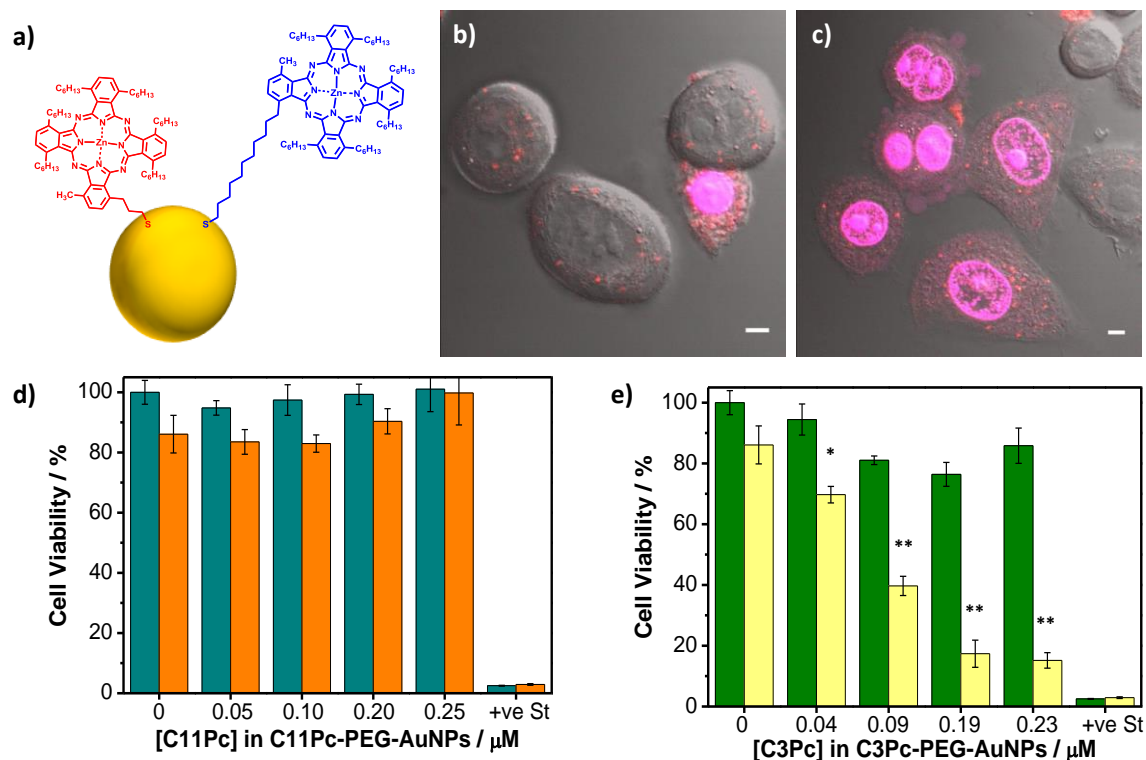


Figure 3. (a) Structure of the AuNPs functionalised with either C3Pc (red) or C11Pc (blue). (b-c) Confocal fluorescence microscopy images of SK-BR-3 cells incubated with either (b) C11Pc-PEG-AuNPs or (c) C3Pc-PEG-AuNPs after irradiation with a 633 nm laser for 6 min. Images are the composite of differential interference contrast (DIC), fluorescence from either C11Pc or C3Pc collected in the red channel ($\lambda_{\text{ex}} = 633 \text{ nm}$; above 650 nm) and fluorescence from propidium iodide collected in the pink channel ($\lambda_{\text{ex}} = 543 \text{ nm}$; 560-615 nm). Scale bars 5 μm . (d-e) CellTiter-Blue[®] cell viability assay for SK-BR-3 cells incubated with (d) C11Pc-PEG-AuNPs or (e) C3Pc-PEG-AuNPs. Cells were either irradiated with a 633 nm HeNe laser (d) orange, (e) yellow) or non-irradiated (d) dark cyan, (e) green). Staurosporine (+ve St) was used as a positive control for cytotoxicity *via* apoptosis. Error bars represent the SD ($n = 3$) within a 95 % confidence interval. Statistically significant difference between C11Pc-PEG-AuNPs and C3Pc-PEG-AuNPs is indicated by * at $P < 0.008$ and ** at $P < 0.0001$, obtained using a two-tailed Student's *t*-test, where $P < 0.05$ is considered statistically significant. Image adapted from García Calavia *et al.*¹⁰ with permission from the European Society for Photobiology, the European Photochemistry Association and the Royal Society of Chemistry.

Conjugation *via* a thiolated linker

The S-Au bond can also be used to conjugate linkers to which the photosensitisers are then attached. The use of such thiolated linkers can avoid the specific synthesis or modification of photosensitisers to introduce a thiol into their structure.

The use of thiolated PEG and other polymers

The use of PEG as one such linker has been reported by several groups.^{14–16} Wang *et al.* reported the combination of PDT and plasmonic photothermal therapy (PTT) using 54 nm gold nanostars functionalised with a thiolated PEG, to which the photosensitiser chlorin e6 was attached *via* EDC (N-(3-Dimethylaminopropyl)-N'-ethylcarbodiimide hydrochloride)-NHS (N-hydroxysuccinimide) chemistry.¹⁴ The use of a 671 nm laser induced the production of singlet oxygen by the chlorin e6 and simultaneously heated the functionalised nanostars, due to the PTT effect. The combination of the chlorin e6 with the nanomaterial not only induced a 75 % increase in the production of $^1\text{O}_2$ as compared to the free chlorin e6, it also allowed for the double therapy effect *via* PDT and PTT. Internalisation of the functionalised nanostars by breast cancer and lung cancer cells was efficient, leading to a high PDT effect. The improved internalisation was correlated with the inhibition of tumour growth *in vivo* in breast tumour-bearing mice. The combination of PDT and PTT for an enhanced tumour destruction was also performed using pH-responsive gold nanorods (AuNRs).¹⁷ Zhang *et al.* synthesised PEGylated AuNRs, to which chlorin e6 was conjugated *via* a hydrazone. The stability of such hydrazone bond is pH dependent and can be easily cleaved at acidic conditions. The chlorin e6 loses its fluorescence when it is conjugated to the AuNRs. However, upon cellular internalisation, the acidic environment inside the cells cleaves the hydrazone bond thus releasing the chlorin e6, which then regains its fluorescent properties. The chlorin e6 is only released when it reaches the acidic environment within the tumour tissue. At this point, PDT can be applied *via* chlorin e6 using a 664 nm wavelength, together with PTT *via* the AuNRs using a 808 nm wavelength. As reported in the previous study,¹⁴ the use of PDT/PTT enhanced the cytotoxicity and the inhibition of tumour growth than an individual therapy by itself.¹⁷ One of the reasons for the enhanced cell kill using the combination therapy is that, during PDT, the oxygen in the tumour tissue is consumed by the treatment itself, leading to hypoxia and thus limiting the potential of the therapy. The use of PDT in conjunction with PTT can solve this problem as, following consumption of molecular oxygen in the tissue, PTT becomes the main therapy thus increasing the tumour killing effect.¹⁴

Kolemen *et al.* reported another system with the potential to solve the hypoxia limitation of PDT.¹⁵ The authors used non-conventional chemical photosensitisers, endoperoxides of arenes, which lead to the production of $^1\text{O}_2$ upon heating *via* controlled cycloreversion. Anthracene-based endoperoxides were conjugated to a thiolated PEG through an amide bond, which was then self-assembled onto the surface of gold nanorods. The irradiation of the functionalised AuNRs with 808 nm wavelength for 10 minutes was sufficient to induce *ca.* 80 % cell death in HeLa cells. A further advantage of the use of endoperoxides as

photosensitisers is their irradiation with NIR light, which can penetrate deeper than commonly used red light into biological tissue, thus opening the possibility to treat deep-lying tumours.¹⁵ In a further attempt to increase light penetration into the tissue, Clement *et al.* attempted the use of X-ray irradiation for PDT.¹⁶ The photosensitiser verteporfin was electrostatically attached to a thiolated PEG on the surface of 12 nm AuNPs. The use of X-ray irradiation did not lead to an increase in PDT efficiency in pancreatic cancer cells, as was seen when the cells were irradiated with a 690 nm laser. The authors claimed that the combination of X-ray and 690 nm irradiation could hold the potential to actively treat deep-lying tumours but further studies are required to confirm these claims.¹⁶

Thiolated polymers other than PEG have also been studied for the conjugation of photosensitisers to gold nanomaterials.^{18,19} Gamaleia *et al.* studied the conjugation of haematoporphyrin to 15 and 45 nm AuNPs *via* polyvinylpyrrolidone.¹⁸ Leukemia cells were treated with the haematoporphyrin-functionalised AuNPs and subjected to 635 nm PDT. Both conjugates were shown to increase the PDT effect as compared to the free photosensitiser, with the 45 nm sized AuNPs performing best.¹⁸ As previously mentioned, PDT can be combined with other therapies including photothermal therapy (PTT). Hollow gold nanospheres (HAuNS) have been functionalised with branched polyethylenimine (PEI), to which the photosensitiser indocyanine green (ICG) was covalently attached.¹⁹ The conjugation of ICG on the HAuNS allowed for their stability in aqueous solutions and, more importantly, it improved the absorption of the system within the NIR region. The increased NIR absorption is advantageous for an enhanced PTT effect. The as-prepared ICG-PEI-HAuNS were tested *in vitro* in 2D and 3D human ovarian carcinoma tumour models, as well as *in vivo* in mice bearing either colon carcinoma CT26 cells or metastatic melanoma B16 cells. All studies suggested that the combination of PDT with PTT showed significantly better results than the use of either single therapy. The *in vitro* studies in 2D models showed a moderate improvement of PTT/PDT efficacy using the ICG-PEI-HAuNS as compared to the free ICG. Additionally, the 3D models showed significant tumour reduction, even though the percentage of cell kill was not as high as in 2D models. The use of the conjugates *in vivo* showed selective accumulation within the tumour tissue and 100 % survival of the treated mice until day 40, a considerable improvement to the mice treated with only ICG or only HAuNS, which survived until days 28 and 32, respectively. The ICG-PEI-HAuNS were further found to inhibit tumour metastasis *in vivo* by destroying both the cancer cells and the surrounding blood vessels.¹⁹

The use of mercapto moieties

The use of linkers based on mercapto moieties to conjugate AuNPs to photosensitisers has been reported in the literature.^{20–22} The linker 6-mercapto-1-hexanol was self-assembled on

the surface of 7 nm AuNPs by Eshghi *et al.*²⁰ Protoporphyrin IX was then conjugated to the linker *via* N,N'-dicyclohexylcarbodiimide (DCC)-promoted coupling. The AuNPs system allowed the internalisation of the hydrophobic porphyrin photosensitiser by HeLa cervical cancer cells and the PDT effect was confirmed with red light irradiation at 630 nm.²⁰ Other research groups have chosen mercaptopropionic acid as the linker for the conjugation of photosensitisers to the AuNP core.^{21,22} A *meso*-tetrahydroxyphenylchlorin (mTHPC) was attached to mercaptopropionic acid self-assembled on 12 nm AuNPs through esterification between the hydroxyl groups of mTHPC and the carboxyl group of the mercaptopropionic acid.²¹ The authors confirmed the PDT potential of the water-soluble mTHPC-functionalised AuNPs *in vitro* using neuroblastoma cells. The combination of the mTHPC with the AuNPs was shown to induce less dark toxicity to the cells than the free mTHPC, thus allowing for the application of higher drug doses for enhanced PDT without leading to any side-toxicity in the absence of light. The major disadvantage of this system was the long irradiation times needed, of up to 1 h, to reach high levels of cell death, which could prove problematic for *in vivo* clinical applications.²¹ In another system, AuNPs were functionalised with porphyrin-brucine photosensitiser conjugates *via* 3-mercaptopropionic acid.²² This system had a different outcome to what was described previously. *In vitro* studies in basaloid squamous carcinoma cells showed a lower efficiency of the functionalised AuNPs as compared to the free photosensitisers, which was attributed to the aggregation of the AuNPs in aqueous media. On the contrary, *in vivo* studies showed efficient PDT leading to tumour reduction in the mice treated with the functionalised AuNPs. The authors suggested that the good effect *in vivo* was due to the interactions of the functionalised AuNPs with plasma proteins, such as human serum albumin (HSA), which led to the generation of supramolecular complexes, thought to enhance PDT.²²

Other thiolated linkers

The conjugation of photosensitisers via alternative thiolated linkers has been widely explored. The selected linkers include multidentate passivant ligands,²³ cysteine,²⁴ thiourea,²⁵ glutathione,²⁶ lipoic acid,²⁷ and imidazole containing linkers.²⁸

The use of multidentate passivant ligands for the conjugation of a porphyrin to AuNPs was explored by Ohyama *et al.*²³ It has been reported that such passivant ligands have the ability to stabilise AuNPs as a substitute to the commonly used citrate or TOAB stabilisers. The authors synthesised a porphyrin-based tetradentate passivant, consisting of four sulfur atoms which can be self-assembled onto the surface of the AuNPs. The presence of the four sulfur-Au bonds allows for the creation of a horizontal porphyrin monolayer around the AuNPs. This type of surface-engineered photosensitiser coated AuNPs are promising PDT agents but their

in vitro or *in vivo* efficacy has yet to be evaluated.²³ More commonly used linkers include cysteine, thiourea and glutathione. Cysteine self-assembled onto the surface of AuNPs can be covalently conjugated to photosensitisers, such as protoporphyrin IX (PpIX), inducing up to 59 % cell death for spermatogonial cells upon irradiation at 633 nm.²⁴ Additionally, the use of a cysteine linker opens the possibility to conjugate the cysteine to other molecules, such as targeting ligands for selective PDT, which will be reviewed later in this article. Vieira *et al.* used thiourea as the linker between 18 nm AuNPs and chlorin e6, using EDC-NHS coupling for the interaction between the linker and the photosensitiser.²⁵ The system was shown to be efficient following 4 h incubation with breast carcinoma cells and PDT at 660 nm, leading to higher levels of cell death than the free chlorin e6 in solution.²⁵ Hari *et al.* developed water-stable 14 nm chitosan reduced AuNPs functionalised with glutathione, which was electrostatically bound to the photosensitiser acridine orange.²⁶ The high loading of photosensitiser yielded highly fluorescent AuNPs conjugates with an enhanced PDT effect *in vitro*. The irradiation at 492 nm induced not only the production of singlet oxygen *via* activation of the acridine orange, but it was also reported that an increase in temperature was induced with the AuNPs acting as the photothermal agents. Therefore, it was suggested that this nanoplatform can be used for a dual PDT/PTT therapy.²⁶

The Pérez-García group has developed several nanoplatforms with non-conventional linkers for the conjugation of photosensitisers for PDT.^{27,28} The group studied the photodynamic effect of three gold-based nanoplatforms, differing in size and shape, conjugated to porphyrin photosensitisers *via* a lipoic acid linker.²⁷ The nanoplatforms of choice were AuNPs, cobalt-nickel nanorods covered with a gold shell (NRs) and hexahedral Janus microparticles (μ P) with two surfaces, gold and polysilicon. The geometric areas of each platform were, respectively, $3.1 \times 10^{-4} \mu\text{m}^2$, $1.3 \mu\text{m}^2$ and $9 \mu\text{m}^2$. The lipoic acid linker was self-assembled onto the gold surface of the nanoplatforms, to which porphyrin photosensitisers were attached through amide bonds. To induce water solubility, the AuNPs and NRs were additionally functionalised with 11-mercaptoundecyl)hexa(ethylene glycol) (MHEG), a PEG derivative. The μ P were functionalised with 6-{2-[2-(2-methoxyethoxy) ethoxy]ethoxy}hexyl) trimethoxysilane (MTMS) on the polysilicon surface, which allowed for the dispersion of the μ P in aqueous solutions. The size and shape of the nanoplatforms was found to play a key role in the PDT efficacy *in vitro*. The NRs were subjected to intrinsic toxicity and their magnetism induced aggregation, thus lowering the efficacy of PDT. The μ P were internalised in smaller amounts than the other nanoplatforms, due to their large size. However, the large size was advantageous as it included more porphyrins per particle than the smaller sized-AuNPs, translating into a good PDT effect. Nevertheless, it was the AuNPs that induced the best

photocytotoxicity *in vitro*, thus concluding that the smaller size was beneficial for cell internalisation and also PDT.²⁷

In a more recent study, Pérez-García and co-workers conjugated zinc porphyrins to the surface of AuNPs *via* zinc-imidazole axial coordination.²⁸ The surface of 7 nm AuNPs was engineered to contain a thiolated PEG ligand, to induce water solubility, and a thiolated 1-(11-mercaptopundecyl)imidazole (Im-C₁₁-SH). The zinc porphyrin Zn(II)meso-tetrakis(4-carboxyphenyl)porphyrin was conjugated to the AuNPs *via* a Zn-imidazole coordinative bond. The conjugation of the porphyrin in this way allows it to adopt a horizontal orientation relative to the surface of the AuNPs, which can be advantageous to avoid the formation of aggregates since it reduces the maximum number of porphyrins that can be incorporated into the system. The formation of the porphyrin-imidazole functionalised AuNPs highly increased the production of reactive oxygen species as compared to the free porphyrin in solution. Additionally, *in vitro* PDT studies with 30 min irradiation using wavelengths between 400-500 nm induced up to 80 % cell death with a concentration of 1.75 μ M of porphyrin within the nanosystem. The use of imidazole coordination provides a simple and stable coordinate bond, in contrast to the commonly used covalent bonds, and holds great potential for future *in vivo* PDT studies since numerous photosensitisers can be readily coordinated to the AuNPs without the need for specialist synthesis of anchor moieties.²⁸

The use of the N-Au bond

Conjugation between AuNPs and photosensitisers *via* N-Au bonds has been particularly studied by the Burda group.^{29–31} The N-Au is a weak bond, with a bond energy of 6 kcal/mol, in comparison with the S-Au bond, which has a bond energy of 47 kcal/mol.²⁹ Therefore, the functionalisation of AuNPs with photosensitisers using the N-Au bond requires other stabilising ligands, such as PEG derivatives. Burda and co-workers developed 5 nm AuNPs functionalised with a thiolated PEG and attached to the terminal amine on a silicon phthalocyanine 4 (Pc4) axial ligand through a N-Au bond. The presence of PEG provides steric repulsion between AuNPs and also enables the stabilisation of the Pc4 on the AuNPs *via* van der Waals interactions. Therefore, the Pc4 is entrapped in what the authors define as a ‘cage-type structure’, allowing the solubilisation of the hydrophobic drug in aqueous solutions. A further advantage of the use of PEG is the low protein adsorption and increased circulation time in the serum, which is essential for PDT.^{1,30} Given the van der Waals interactions between PEG and Pc4 on the surface of the AuNPs, the photosensitiser is forced to adopt a horizontal orientation relative to the Au core. While this orientation can potentially enable up to 100 Pc4 molecules per AuNP, only 30 Pc4 molecules were conjugated.^{29,30} The mechanism of action of

the synthesised nanosystem consists on the selective delivery of the drug to the tumour tissue *via* the enhanced permeability and retention effect (EPR). Upon delivery towards the tumour tissue, Pc4 is released from the AuNPs due to the attraction of the hydrophobic Pc4 to the lipid bilayers of the cell membrane and the weak binding between Pc4 and the AuNPs. The release of the drug is beneficial since, upon conjugation with the AuNPs the fluorescence of Pc4 is slightly quenched. The release of Pc4 allows for the recovery of the fluorescence. While Pc4 is internalised by the cancer cells, the AuNPs remain in the extracellular space. *In vitro* studies showed that, upon internalisation, Pc4 moves towards the mitochondria leading to remarkable PDT effects.³⁰

The Pc4-PEG-AuNPs were evaluated *in vivo* to investigate both the PDT effect in animal tissues and the pharmacokinetics and excretion from the body.^{29,31} The most important advantage of the use of Pc4-PEG-AuNPs *versus* free Pc4 is the length of time it takes the drug to reach the tumour tissue, which can be reduced from *ca.* 48 h to less than 2 h when conjugated to the AuNPs.²⁹ The fate of the Pc4 and the PEGylated AuNPs within the body was studied over a 7-day period. Even though the Pc4 and the AuNPs followed different routes and accumulated in different organs, both components were found to be excreted *via* the renal and hepatobiliary systems.^{29,31} The Burda group has broadened these studies by introducing biological ligands for targeted PDT, which will be discussed later.

Electrostatic interaction

Photosensitisers can be conjugated to charged, either positively or negatively, gold nanoparticles. Several research groups have shown the advantages of using such conjugation for PDT.^{11,32–36} The effect of the size of AuNPs electrostatically bound to the photosensitiser PpIX was studied with AuNPs of diameters 19, 66 and 106 nm.³² Cationic AuNPs were synthesised with branched polyethyleneimine (BPEI) reduction, which were functionalised with the negatively charged PpIX. The authors found that, in solution, the larger sized AuNPs correlated with an increased production of singlet oxygen. Furthermore, *in vitro* studies in MDA-MB-231 human breast adenocarcinoma cells showed that the larger AuNPs (106 nm) were not as easily internalised by the cells as the smaller AuNPs (19 and 66 nm). As a result, the 66 nm AuNPs induced the highest intracellular production of ROS. While the free PpIX in solution was only able to kill 22.6 % of the cells treated with 532 nm PDT, the attachment of PpIX on the surface of either of the AuNPs (16, 66 or 106 nm) induced over 50 % cell death post-PDT. The higher intracellular uptake and higher production of singlet oxygen by the 66 nm AuNPs was associated with the highest cell death *in vitro*.³²

The compound 5-aminolevulinic acid (5ALA) is commonly used in PDT since it is a natural precursor of the photosensitiser PpIX produced during the biosynthesis of haem.¹ The electrostatic conjugation of 5ALA to AuNPs has been reported with promising results for PDT.^{33,34} Xu *et al.* synthesised 24 nm AuNPs functionalised with BPEI and 5ALA in a similar manner as reported above for the conjugation of PpIX to AuNPs.³³ The authors tested their conjugates *in vitro* using K562 chronic myelogenous leukaemia cells and found that the AuNPs enhanced the singlet oxygen production and intracellular uptake of 5ALA. Additionally, enhanced selectivity towards tumour cells, due to the positively charged AuNPs, which are attracted to cancer cells given their higher negative-zeta potential than healthy cells, was reported. An incubation time of 4-6 hours combined with green light irradiation was shown to be ideal for PDT, given the low intrinsic toxicity of the green light itself.³³ Similar results were obtained by Mohammadi *et al.* in Mel-Rm metastatic melanoma cells.³⁴ The combination of 5ALA with AuNPs was found to be advantageous since lower concentrations of the 5ALA on AuNPs lead to the same phototoxicity than higher concentrations of unconjugated 5ALA, thus limiting the potential damage of high concentrations of 5ALA on healthy cells.³⁴

The use of MEF, previously discussed for AuNPs functionalised with thiolated photosensitisers, has also been studied for electrostatically bound drugs. Huang *et al.* conjugated CTAB stabilised-AuNRs with chlorin e6 through electrostatic interactions.¹¹ The authors proved that the close distance between AuNRs and chlorin e6 enhanced the fluorescence of the photosensitiser. The increase in fluorescence correlated with an improved production of singlet oxygen and thus it translated into three times more efficient PDT *in vitro* as compared to free chlorin e6.¹¹

Electrostatic conjugation of photosensitisers to AuNRs has also been reported for combined PDT/PTT therapies.^{35,36} Jang *et al.* synthesised cetyltrimethylammonium bromide (CTAB) coated AuNRs, further functionalised with a thiolated PEG and a thiolated positively charged peptide, to which the negatively charged photosensitiser Al(III) phthalocyanine chloride tetrasulfonic acid (AlPcS₄) was electrostatically attached.³⁵ The fluorescence of AlPcS₄ was quenched upon conjugation to the AuNRs, but it could be recovered when the drug was released. Up to 80 % of the drug could be released in physiological conditions after 24 h. The combination of AlPcS₄ with AuNRs allowed for effective delivery into cancer cells both *in vitro* and *in vivo*, up to four times higher than for the free photosensitiser. Following internalisation and release of the drug, an enhanced cell death was seen for the AlPcS₄-AuNRs (78 %) as compared to the free AlPcS₄ (36 %). More importantly, the combination of PDT at 670 nm and PTT at 810 nm efficiently inhibited 95 % of the tumour growth *in vivo*, a considerable improvement of the 79 % enhancement when PDT was performed as a single therapy. Despite

the promising results seen, the authors speculated that further optimisation of the PTT conditions could lead to better results.³⁵ The main disadvantage with this method was the need to use two different irradiation wavelengths for PDT and PTT. Bhana *et al.* developed a system where PDT and PTT could be achieved with a single wavelength, 808 nm.³⁶ The authors electrostatically conjugated CTAB-pegylated AuNRs to the photosensitiser silicon 2,3-naphthalocyanine dihydroxide (SiNC), which were stabilised with alkylthiols of different lengths. The alkylthiols used were 6-mercaptohexanoic acid, 11-mercaptopundecanoic acid and 16-mercaptohexadecanoic acid, varying in the length of the carbon atom chain (5, 10 and 15 atoms, respectively). A concentration of 0.5 nM of SiNC induced complete cell destruction regardless of the length of the alkylthiol used. However, at low concentrations of the drug, the PDT/PTT efficiency was enhanced with the longest alkylthiol.³⁶

The group of Pérez-García have investigated the use of amphiphilic gemini-type pyridinium salts for conjugation of porphyrins to AuNPs.³⁷ These types of salts have been described as stabiliser agents for AuNPs.^{38,39} However, this study is the first report of the use of a bis-pyridinium salt (1·2Br) not only to stabilise the AuNPs but also to anchor the photosensitiser *via* electrostatic interactions. The authors functionalised 7-10 nm AuNPs with a mixture of 1·2Br and PEG, to provide aqueous solubility, and an anionic porphyrin as the photosensitiser. The nanosystem was shown to hold great potential for PDT since SK-BR-3 human breast adenocarcinoma cells were more highly damaged than non-tumorigenic mammary epithelial MCF-10A cells.³⁷

Conjugation to silica coated gold nanomaterials

The conjugation of photosensitisers can be achieved through encapsulation in a silica shell surrounding a gold nanocore, as reported by various research groups.^{40,41} Silica coated gold nanoplatfoms haven been used not only for PDT and combination therapies, but also to include surface-enhanced Raman scattering (SERS) detection and imaging of tumour tissue.⁴⁰ Gold nanostars have been coated with 3,3'-diethylthiatricarbocyanine iodide (DTCC) as the SERS tag, and then covered with a mesoporous silica shell into which the photosensitiser methylene blue was encapsulated. The use of gold nanostars is not arbitrary since they induce better SERS enhancement than conventionally used spherical AuNPs. SERS-enhanced imaging was performed using a 785 nm wavelength, while the PDT treatment was performed by irradiating the methylene blue in the nanosystem using 633 nm light. The combination of DTCC and methylene blue in the same system was advantageous for the development of theranostics, by which diagnosis (*via* SERS imaging) and therapy (*via* singlet oxygen generation during PDT) can be simultaneously performed.⁴⁰ Seo *et al.* developed a similar system, based

on pegylated gold nanorods (AuNRs) coated with a silica shell in which methylene blue was embedded *via* physical adsorption.⁴¹ The substitution of gold nanostars by AuNRs can be advantageous since it opens the possibility to add the additional therapy of PTT. Irradiation with a single NIR wavelength, 780 nm for 50 minutes, was sufficient to induce combined PDT and PTT damage, together with SERS imaging for theranostic applications. The improvement in cell death through the combination of PDT and PTT was confirmed by the levels of cell death for bare AuNRs, 69 %, as compared to the methylene blue-silica-coated AuNRs, 89 %.⁴¹ Therefore, this system is a promising alternative for theranostics in cancer treatment. The covalent conjugation of silica coated gold nanoclusters with chlorin e6 *via* EDC/NHS coupling has been reported for fluorescence imaging-guided PDT.⁴² Covalent conjugation of a photosensitiser to silica coated gold nanoclusters was found to have several advantages including a high loading of the drug (14.6 wt%), no leakage of the photosensitiser during circulation in the serum and enhanced PDT damage at 671 nm leading to efficient inhibition of tumour growth *in vivo*.⁴²

In a somewhat different system, silica nanoparticles containing a gold core have been reported for PDT/PTT combination therapy.⁴³ Ricciardi *et al.* have synthesised *ca.* 40 nm silica nanoparticles in which a cyclometalated iridium (III) complex (Ir_1) was embedded. Additionally, the silica nanoparticles contained a gold core ($\text{Ir}_1\text{-AuSiO}_2$). The conjugation of Ir_1 to the AuSiO_2 nanoparticles produced a decrease in the singlet oxygen quantum yield from 0.97 for the free Ir_1 to 0.22 for the $\text{Ir}_1\text{-AuSiO}_2$. However, U87MG glioblastoma cells internalised the conjugate (Ir-AuSiO_2) more efficiently than the free Ir_1 , thus cell death was enhanced upon conjugation of Ir_1 to the AuSiO_2 . Light irradiation for combined PDT/PTT was performed *via* 700 nm two photon excitation, able to reach deep-lying tumours. More importantly, the introduction of the gold core in the silica nanoparticles was found to be key for an enhanced tumour destruction at lower concentrations of the drug.⁴³ The nanoplatform presented in this study holds potential for the development of a highly efficient, deep-penetration cancer therapy.

Alternative conjugation methods for gold-mediated PDT

The development of other conjugation methods and platforms based on gold by which efficient PDT can be achieved have also been reported in the literature.^{44–49} Hu *et al.* used a LayerbyLayer (LbL) method to assemble the photosensitiser Al(III) phthalocyanine chloride tetrasulfonic acid (AlPcS_4) onto gold nanorings.⁴⁴ In this case, LbL assembly consists of successive deposition of layers of the photosensitiser around the gold. The authors synthesised gold nanorings covered with a layer of thiolated PEG. A layer of a cationic

polymer, poly(allylamine hydrochloride) (PAH), was then added to allow for the electrostatic interaction with the photosensitiser, a layer of which was added on top of the PAH. A second layer of PAH followed by ALPcS₄ was attached, creating a system with two full layers of photosensitiser. The conjugation of the photosensitiser with gold induced a quenching effect, as seen in many systems reported in this review. However, upon internalisation by the cells, the ALPcS₄ drug was efficiently released, regaining its fluorescence and ability to produce ROS. The addition of the second ALPcS₄ layer was key for an enhancement in PDT relative to the free photosensitiser, reaching levels of up to 85 % cell death following 6 h incubation with MDA-MB-231 breast cancer cells and NIR irradiation for ROS generation.⁴⁴

Other studies have shown alternative nanosystems. Cui *et al.* developed a gold cluster nanoassembly.⁴⁵ The conjugation of BSA and cysteine-stabilised gold nanoclusters with glutathione resulted in the cleavage of the BSA intramolecular disulfide bonds and the formation of new intermolecular disulfide bonds, thus creating a nanoassembly of many gold nanoclusters coming together. The nanoassembly itself was also used as the photosensitiser. The use of the nanoassembly showed an improvement in PDT efficacy as compared to the single gold nanoclusters. However, only moderate levels of cell death were achieved, considerably less than other systems described in this review.⁴⁵ In a recent report, Yan *et al.* have developed a system based on AuNRs and chlorin e6.⁴⁶ The surface of 70×17 nm AuNRs was modified with poly(styrene sulfonate) (PSS) and the chlorin e6 was conjugated to branched PEI, both polymers used for an increased stability in aqueous solutions. The PSS-AuNRs and PEI-Chlorin e6 are not directly attached to one another, but they are both assembled onto a template, which the authors refer to as a 'plaster'. The presence of the AuNRs and chlorin e6 on such a plaster allows for combined PTT (808 nm) and PDT (660 nm), leading to complete tumour destruction following 16 days after treatment *in vivo*. Such a plaster system is advantageous since it is non-invasive and can be used in numerous occasions to treat tumours. However, its application is limited to superficial tumour lesions due to the nature of the plaster application.⁴⁶

Other nanoparticle systems all supported by gold include liposomes loaded with AuNPs,⁴⁷ carboxymethyl dextran nanoparticles stabilised with gold,⁴⁸ and the use of a thin shell of gold comprised of a gold sulfide (Au₂S) dielectric core.⁴⁹ Liposomes loaded with 3-5 nm AuNPs and the photosensitiser Rose Bengal were particularly efficient for PDT combined with chemotherapy, when the chemotherapeutic drug doxorubicin was included within the system.⁴⁷ The use of gold to stabilise carboxymethyl dextran nanoparticles loaded with the photosensitiser chlorin e6 was advantageous since it increased the tumour selectivity and thus the PDT effect *in vivo*.⁴⁸ Finally, the physical adsorption of gold-sulfide gold (Au-Au₂S)

with the photosensitiser ICG was found to be a promising alternative for NIR-PDT/PTT given the non-toxic nature of Au-Au₂S and their easy internalisation by tumorigenic cells.⁴⁹

AuNPs should not only be considered as nanocarriers for the delivery of photosensitisers but can be used as the phototoxic agents themselves. El-Hussein *et al.*⁵⁰ have shown the uptake and phototoxicity of 50 nm diameter AuNPs on MCF-7 and A549 cancer cells upon laser irradiation. The cytotoxicity observed was similar to that of a laser activated phthalocyanine used as control, although the cytotoxicity was not as efficient as that induced by non-functionalised silver nanoparticles, which can also be used as phototoxic agents themselves.⁵⁰

Actively targeted PDT

The nanoparticle systems described above typically rely on the enhanced permeability and retention (EPR) effect for selective accumulation within the tumour tissue, known as passive targeting. The EPR effect is related to the creation of abnormal, leaky and loosely-connected blood vessels in the tumour tissue *via* angiogenesis and the lack of lymphatic drainage in the tumour interstitial fluid, responsible for the nanoparticles permeating and being retained.⁵¹ The use of gold nanoparticles provides the opportunity to additionally use biological ligands in order to further increase the selectivity towards tumours, *i.e.*, active targeting. Targeting ligands are responsible for the selective interaction between the nanoparticles and specific receptors overexpressed on the surface of tumour cells, but not healthy cells, thus increasing internalisation.⁵² **Figure 4a** shows the receptors that have been targeted, in different cancer cells, using gold nanoparticles. The most commonly targeted receptors include the epidermal growth factor receptors 1 (EGFR) and 2 (HER2), $\alpha\text{v}\beta$ integrins, the transferrin receptor, nucleolin, the folate receptor, cluster determinants 44 (CD44), and the aberrant glycosylation on cancer cells, including overexpressed carbohydrates and endogenous lectins.¹ Gold nanoparticles can be functionalised with ligands that selectively target these receptors. The reported targeting ligands conjugated to gold nanoparticles for PDT that will be reviewed in this paper include antibodies, carbohydrates and lectins, peptides, aptamers, folic acid and hyaluronic acid (**Figure 4b**).

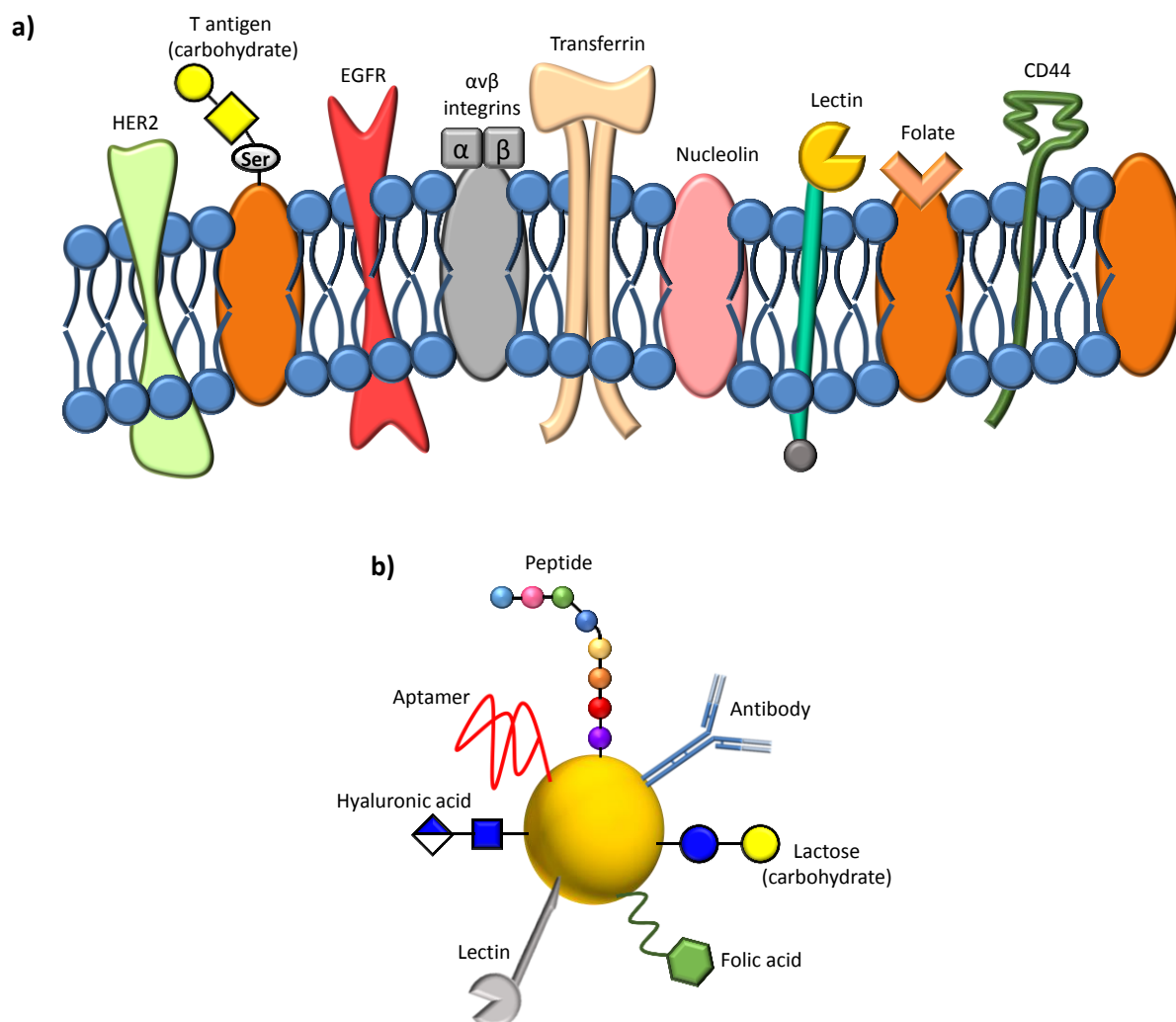


Figure 4. (a) Schematic representation of a cell membrane, showing some of the overexpressed cancer cell receptors that can be used for selective targeting. It should be noted that these receptors are not all present in all cancer cell types. **(b)** Schematic representation of a gold nanoparticle functionalised with the ligands that are commonly used to target overexpressed receptors on cancer cells. It should be noted that these ligands are not all present in the same nanoparticle. Image **(a)** was adapted from García Calavia and Russell¹ with permission from the European Society for Photobiology, the European Photochemistry Association and the Royal Society of Chemistry.

Antibodies

The most commonly reported biological ligand used for targeting PDT is antibodies. Antibodies have a strong binding affinity towards their antigen of interest, with dissociation constants (k_d) within the 10^{-8} - 10^{-12} M range.⁵³ Several studies have reported the conjugation of antibodies to PEGylated AuNPs using EDC-NHS coupling to the terminal carboxylic acid of

the PEG chain.^{54–56} As previously described, Russell and co-workers synthesised stable C11Pc-PEG-AuNPs with good photodynamic toxicity *in vitro* and *in vivo*. The group further increased the selectivity of the C11Pc-PEG-AuNPs to breast cancer cells using anti-HER2 antibodies. The HER2 receptor is found overexpressed in *ca.* 10–34 % of aggressive breast cancers, thus becoming an important target for selective PDT.⁵⁴ Stuchinskaya *et al.* prepared the four-component anti-HER2 antibody-C11Pc-PEG-AuNPs (**Figure 5a**) and showed that the addition of the antibody did not alter the ability of the nanoparticles to produce singlet oxygen.⁵⁵ The authors confirmed the importance of the antibody to achieve high selectivity by comparing three mammary cell lines; HER2 positive SK-BR-3 human breast adenocarcinoma cells, HER2 negative MDA-MB-231 human breast adenocarcinoma cells and non-tumorigenic MCF-10A human mammary epithelial cells. *In vitro* PDT studies using an irradiation wavelength of 633 nm showed apoptotic cell death levels of 60 % for SK-BR-3 cells, 25 % for MDA-MB-231 cells and 7 % for MCF-10A cells, indicating that the selective interaction between anti-HER2 antibody and the HER2 receptor on the surface of SK-BR-3 cells leads to an increased internalisation and thus enhanced PDT efficacy.⁵⁵ The reported anti-HER2 antibody-C11Pc-PEG-AuNPs were shown to be internalised efficiently, initially locating around the cell membrane (**Figure 5b**) and moving towards the acidic organelles, *i.e.*, the lysosomes, over time (**Figure 5c**), leading to efficient cell death (**Figure 5d**). In a more recent study, Penon *et al.* synthesised water-stable AuNPs functionalised with a thiolated porphyrin derivative as the photosensitiser, and PEG as the stabilising agent to induce water solubility.⁵⁶ Anti-HER2 antibody was further conjugated to the system through the PEG and SK-BR-3 cells were targeted *in vitro*. Irradiation of the cells between 530–585 nm using a fluorescence microscope allowed the visualisation of cell death using the dead cell marker propidium iodide.⁵⁶

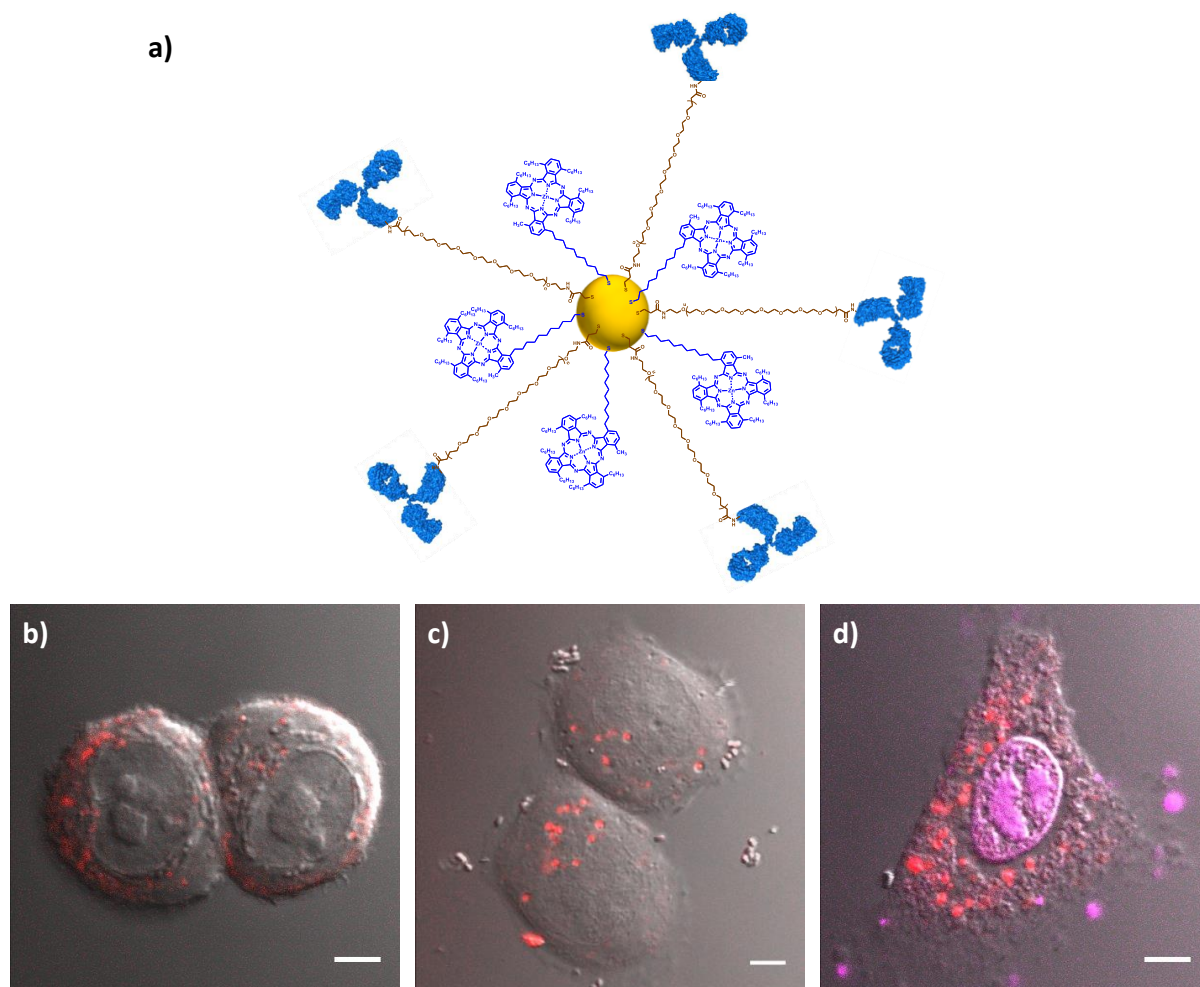


Figure 5. (a) Schematic representation of the anti-HER2 antibody functionalised C11Pc-PEG-AuNPs. (b-d) Confocal fluorescence microscopy images of SK-BR-3 cells incubated with anti-HER2 antibody functionalised C11Pc-PEG-AuNPs either before irradiation (b-c), right after incubation (b) or 19 h after incubation (c), or after irradiation (d) with a 633 nm laser for 6 min. Images are the composite of differential interference contrast (DIC), fluorescence from C11Pc collected in the red channel ($\lambda_{\text{ex}} = 633 \text{ nm}$; above 650 nm) and fluorescence from propidium iodide collected in the pink channel ($\lambda_{\text{ex}} = 543 \text{ nm}$; 560-615 nm). Scale bars 5 μm .

The human epidermal growth factor receptor 1, also known as EGFR, has also been widely targeted *via* antibodies.^{57–60} Kuo and co-workers synthesised CTAB-stabilised AuNRs (35 nm \times 9.3 nm in size) conjugated to poly(styrene-altmaleic acid) (PSMA), to which the photosensitiser ICG was electrostatically attached.⁵⁷ Additionally, the negatively charged ICG was functionalised with anti-EGFR antibodies electrostatically, due to the presence of positively charged antibody fragments. The combination of the AuNRs with ICG was optimal for the combined action of PDT and PTT following NIR irradiation at 808 nm. The antibody-ICG-functionalised AuNRs were found to induce no damage to A549 lung carcinoma cells in

the absence of light but killed up to 98 % cells upon irradiation.⁵⁷ The authors further broadened their study by investigating the use of AuNPs instead of AuNRs. The functionalisation of AuNPs with branched PEI, electrostatically conjugated to ICG and anti-EGFR antibodies, was also found to be useful for combined PDT/PTT. However, the size of the AuNPs core was key for efficacy of the treatment, with larger AuNPs inducing a better photochemical effect. The sizes of AuNPs studied were 13 nm, 50 nm and 100 nm, which induced, respectively, 66 %, 80 % and 92 % cell death following treatment.⁵⁸

The Kiang group has also reported the use of anti-EGFR antibodies for targeted PDT.^{59,60} This research group focuses on the synthesis of gold nanorings functionalised with a thiolated PEG, a sulfonated aluminium phthalocyanine (AlPcS) and a 16-mercaptohexadecanoic acid, acting as the linker to anti-EGFR antibodies. The group was able to perform PDT in combination with PTT using an irradiation wavelength of 1,064 nm for PTT but also as a two-photon excitation of the AlPcS photosensitiser for PDT, in conjunction with the more conventionally used 660 nm wavelength for the irradiation of phthalocyanines for PDT.^{59,60}

Lectins and carbohydrates

Carbohydrates and lectins, carbohydrate-binding proteins, are both expressed on the surface of all healthy human cells and play important roles in the organism including, but not limited to, cell growth, cell differentiation and adhesion, and cell signalling.⁶¹ The expression of carbohydrates and lectins on the surface of cancer cells can change, leading to over- or under-expression of specific receptors. This aberrant glycosylation in cancer cells presents an opportunity for selectively targeted cancer therapies, including PDT.^{61,62} Such targeted therapies can either use lectins to target glycoconjugates on the surface of cancer cells, or use carbohydrates to target endogenous lectins.⁶¹ Even though the binding affinity between specific lectins and carbohydrates (k_d values between 10^{-3} - 10^{-6} M) is not as high as antibody/antigen interactions, several studies showing effective glycotargeting have been reported.^{53,61,62}

The use of the lectin Jacalin to target the Thomsen-Friedenreich disaccharide (T antigen), overexpressed in over 90 % of primary human carcinomas, has been reported by Russell and co-workers.⁶² C11Pc-PEG-AuNPs were conjugated to Jacalin *via* EDC-NHS coupling to the terminal end of the PEG ligand (**Figure 6a**). Jacalin conjugated and unconjugated C11Pc-PEG-AuNPs were compared for the treatment of HT-29 colon adenocarcinoma cells, which overexpress the T antigen. Jacalin has a high binding affinity towards the T antigen ($k_d = 500 \pm 50$ nM) so it was expected to selectively target HT-29 cells. Indeed, internalisation of the Jacalin conjugated C11Pc-PEG-AuNPs was enhanced (**Figure 6b**) as compared to non-

conjugated C11Pc-PEG-AuNPs (**Figure 6c**). The enhanced internalisation induced high levels of cell death (*ca.* 95-98 %) post-PDT, a marked improvement from the non-conjugated C11Pc-PEG-AuNPs (*ca.* 8 % cell death), which occurred following the necrotic pathway. Visualisation of cell death was confirmed by the dramatic change in cell morphology (**Figure 6d**), as well as the pink staining with the dead cell marker propidium iodide (**Figure 6e**).⁶² The comparison of Jacalin conjugated C11Pc-PEG-AuNPs with anti-HER2 antibody conjugated C11Pc-PEG-AuNPs confirmed the optimal targeting ability of both ligands. While the significant difference between the k_d value for the antibody and the lectin was thought to favour targeting by the antibody, the prevalence of the carbohydrate receptor on the cancer cell surface ensured that both targeting molecules induced comparable levels of phototoxicity in the HT-29 and SK-BR-3 cells.⁵⁴

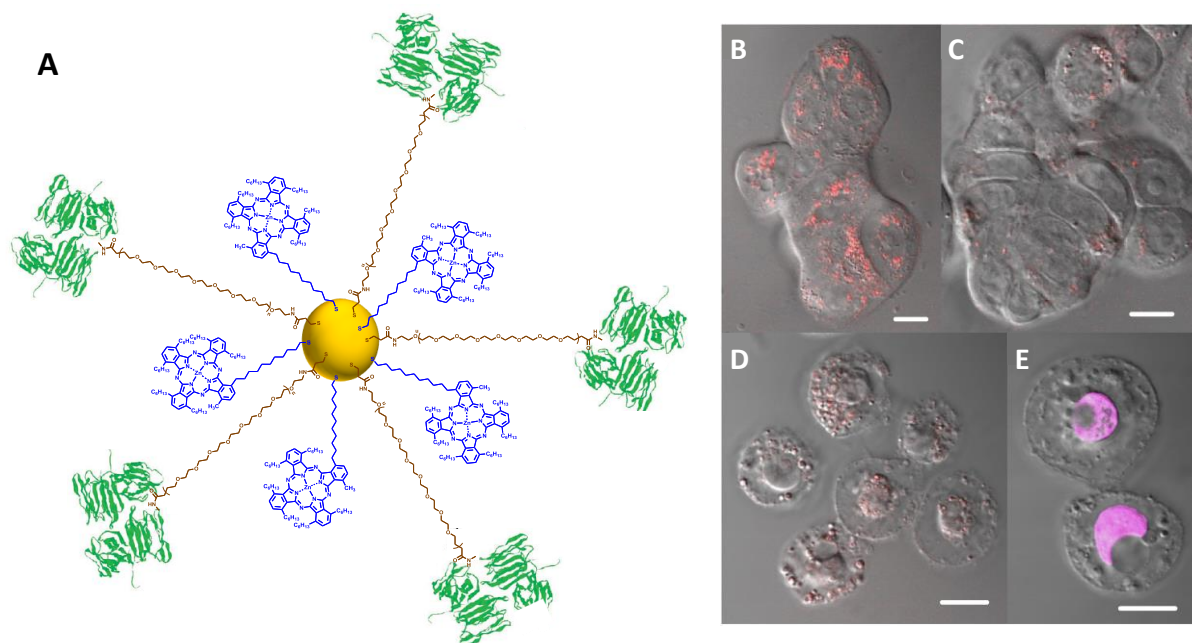


Figure 6. (A) Schematic representation of the Jacalin conjugated C11Pc-PEG-AuNPs used in this study. (B-E) Merged differential interference contrast and confocal fluorescence microscopy images of HT-29 colon adenocarcinoma cells incubated for 4 hours with (B) Jacalin-conjugated nanoparticles (2 μ M C11Pc equivalent) and (C) non-conjugated nanoparticles (2 μ M C11Pc equivalent). (D) After photodynamic therapy treatment, the cell morphology of HT-29 cells incubated with the Jacalin-conjugated nanoparticles dramatically changed, and (E) the HT-29 cells after photodynamic therapy with the Jacalin-conjugated nanoparticles stained positive for propidium iodide (5 mg/mL). Scale bars represent 10 μ m. Figure reproduced from Obaid *et al.*⁶² with permission from John Wiley and Sons © Wiley-VCH.

The Russell group has also reported the use of the carbohydrate lactose to target cancer cells.⁶¹ The authors successfully used a thiolated lactose, self-assembled on the surface of AuNPs, not only as a targeting ligand for PDT, but also as the stabilising agent of the AuNPs in aqueous solutions. The synthesis of AuNPs functionalised with a mixed monolayer of lactose and a C3Pc photosensitiser was reported. The use of the C3Pc photosensitiser was beneficial to induce high levels of singlet oxygen *via* MEF, as discussed above. The conjugated lactose-C3Pc-AuNPs were tested *in vitro* using two different breast cancer cell lines, namely MDA-MB-231 and SK-BR-3 cells. The MDA-MB-231 cells were shown to overexpress galectin-1, a galactose-binding lectin, on their surface and their selective binding to the lactose-C3Pc-AuNPs was shown using an enzyme linked immunosorbent assay (ELISA). However, even though there was a selective interaction between lactose and the galectin-1 on MDA-MB-231 cells and efficient intracellular uptake, there was not an enhanced photodynamic cell kill as compared to control untargeted AuNPs. The second cell line studied, SK-BR-3, did not show an overexpression of galectin-1. Nevertheless, PDT studies confirmed enhanced cell death when the SK-BR-3 cells were treated with lactose-C3Pc-AuNPs (97 % cell death) in comparison with unconjugated control AuNPs (75 % cell death) at a concentration as low as 0.05 μ M following only a 3 h incubation. The selective targeting towards SK-BR-3 cells, that lack galectin-1, can be explained by the presence of other galactoside-binding receptors and suggested the investigation of glucose transporter 1. This study shows the remarkable potential of using carbohydrates for enhanced PDT *in vitro* and *in vivo*.⁶¹

Peptides

The use of peptides for PDT has been increasingly reported. As previously mentioned, the Burda and Broome groups engineered their Pc4-PEG-AuNPs to contain targeting peptides for brain tumours.^{63–66} These groups initially targeted the EGFR overexpressed on the surface of brain cancer cells using EGF peptides, which interact specifically with EGFR ($k_d = 22$ nM).⁶³ As previously described, the Pc4 photosensitiser was attached to the AuNPs *via* a weak N-Au bond stabilised by the presence of PEG. As a result, the Pc4 was entrapped in a ‘cage-like structure’ and its fluorescence was quenched. EGF peptides were then conjugated to the terminal chain of the PEG using EDC-NHS coupling. The effectiveness of these AuNPs relies on the effective release of Pc4 into the cancer cells. The presence of the EGF peptides was shown to enhance the intracellular uptake of Pc4 by a factor of ten. Higher uptake was possible due to a longer interaction between the AuNPs and the cell membrane, which allows more Pc4 to be released into the cells *via* receptor-mediated endocytosis. The endocytosed Pc4 moves towards the endosomes upon internalisation, in contrast with the Pc4 coming from non-targeted AuNPs, which is directed towards the mitochondria.^{63,64} The use of EGF peptides to

target brain tumours was thus beneficial for the development of AuNPs able to cross the blood brain barrier and lead to efficient photodynamic cell kill and tumour reduction.^{63,64} The research was extended by using another peptide, transferrin, to target the transferrin receptor overexpressed in brain tumour malignancies.⁶⁵ The authors conjugated a seven amino acid transferrin sequence to the Pc4-PEG-AuNPs, obtaining an average of 39 peptides per AuNP. *In vitro* studies showed a 2-3 fold improvement in the intracellular uptake of Pc4, which correlated with a good photodynamic efficacy *in vivo*. The main advantage of using transferrin was the ability to efficiently cross the blood-brain-barrier (BBB) and more importantly the possibility to use reduced drug concentrations, up to ten times less, to obtain the same PDT efficacy as that seen with untargeted AuNPs.⁶⁵ Given the promising results seen with both EGF and transferrin peptides, the use of dual targeting was evaluated.⁶⁶ The Pc4-PEG-AuNPs were efficiently conjugated with both EGF and transferrin peptides, and tested *in vitro* and *in vivo*. Even though the dual targeting showed a remarkable improvement over untargeted AuNPs, the improvement was only moderate relative to the single-targeted AuNPs reported above.⁶⁶ The use of the transferrin peptide was also reported by Yu *et al.*⁶⁷ In their study, the authors prepared PSMA polymer coated AuNPs to which a layer of methylene blue was electrostatically attached, followed by EDC-NHS coupling to transferrin. The targeted AuNPs were reported to be internalised three times more efficiently by transferrin-overexpressing HeLa cells as compared to untargeted AuNPs. The higher internalisation correlated with an increased cell death post-PDT, with levels of 30 % for free methylene blue, 45 % for untargeted AuNPs and 65 % for transferrin-targeted AuNPs.⁶⁷ Therefore, the use of either EGF or transferrin peptides has been shown to be highly efficient for the treatment of cancer.

The receptor ephrin type B-receptor 4 (EphB4), a transmembrane protein overexpressed in several tumours, has been targeted using the TNYL (threonine-asparagine-tyrosine-leucine) peptide.⁶⁸ Hollow gold nanospheres were functionalised with a thiolated PEI and a thiolated PEG pre-attached to TNYL peptides. The photosensitiser ICG was then incorporated within the system *via* a dehydration reaction with PEI. The synthesised nanosystem was used for combined PDT/PTT using NIR irradiation. The nanosystem was evaluated *in vitro* using a EphB4 positive cell line, CT-26 mice colon cancer cells, and a EphB4 negative cell line, A549 human lung cancer cells. The internalisation by the cells was found to be higher for CT-26 cells *via* receptor-mediated endocytosis, which localise the targeted nanospheres into the lysosomes. Additionally, *in vivo* studies using Balb/c mice with CT-26 tumours showed that the TNYL targeted nanospheres were more efficient than untargeted nanospheres since, at the same concentration, they require a lower laser power to induce similar PDT effects. More importantly, the authors revealed that the mechanism by which tumours become resistant to

free ICG does not cause a problem for TNYL targeted nanospheres, which are still able to efficiently kill cancer cells.⁶⁸

Several studies have taken advantage of the acidic pH within tumour tissues for drug release.^{69–71} Wu *et al.* used RGD (arginine-glycine-aspartic acid) peptides to specifically target $\alpha v \beta$ integrins overexpressed on the surface of cancer cells.⁶⁹ The authors synthesised 14 nm AuNPs and functionalised them with 5ALA, which is converted to the photosensitiser PpIX, *via* an acid sensitive hydrazone bond, with RGD peptides and with a zwitterionic peptide sequence that provides ‘stealth-like’ properties to avoid protein adsorption. The RGD-5ALA-AuNPs were efficiently internalised by A549 cells, almost four times better than non-targeted 5ALA-AuNPs, confirming the targeting ability of the RGD. The hydrazone bond linking the AuNPs and the 5ALA is broken at acidic conditions, such as the low pH found in tumour tissues. Therefore, 5ALA is released into tumour cells upon internalisation. Even though PDT with RGD-5ALA-AuNPs showed a remarkable improvement from the free 5ALA, the improvement relative to non-targeted 5ALA-AuNPs was only moderate.⁶⁹ In another system, Liu *et al.* prepared gold nanorods (57.3×16.2 nm) covered with a 21 nm mesoporous silica shell, into which the photosensitiser ICG was embedded.⁷⁰ The AuNRs were then functionalised with 3-aminopropyltriethoxysilane (APTES), which could be linked through an amide bond to β -cyclodextrin. The targeting agent in their system was an RLA (arginine-leucine-alanine) peptide, containing mitochondria targeting ability, which was attached to the cyclodextrin *via* host-guest interaction. Finally, a charge-reversible polymer made up of a chitosan oligosaccharide modified with PEG, linked to a 2,3-dimethylmaleic anhydride (DMA) using a weak acid sensitive amide bond, was attached to the AuNRs electrostatically to induce ‘stealth-like’ properties. Similar to the previous study, the acidic environment in the tumour tissue leads to the dissociation of the DMA polymer, allowing the exposure of the RLA peptide, which drives the cellular uptake due to its strong mitochondria targeting ability. Upon internalisation, the conjugates can then be used for combined PDT/PTT using a NIR wavelength of 808 nm. This nanoconjugate was shown to have potential for combination therapies and allows for its functionalisation with other ligands, including chemotherapeutic drugs, to further enhance its tumour destruction ability.⁷⁰

Other important receptors involved in cancer progression, metastasis and angiogenesis are matrix metalloproteinases (MMP), especially MMP2.⁷¹ Xia *et al.* included MMP2 polypeptides in gold nanoclusters in order to target this receptor. Gold nanoclusters coated with glutathione (GSH) of 2 nm in size were functionalised with *cis*-aconitic anhydride modified doxorubicin, a chemotherapeutic drug, and chlorin e6 *via* EDC-NHS coupling and with PEGylated MMP2 polypeptides. The functionalised nanoclusters can be used for fluorescence

imaging combined with PDT and chemotherapy. Chemotherapy occurs when doxorubicin is released from the nanoclusters due to the acidic pH inside the tumours. Fluorescence imaging and PDT were both dependent on the chlorin e6 photosensitiser. The presence of the MMP2 polypeptides allowed for an increased cell internalisation, together with an enhanced tumour destruction *in vivo*.⁷¹

Aptamers

Aptamers are made of single-stranded DNA or RNA oligonucleotides with high affinity towards specific target molecules.⁷² The selectivity towards their target makes them ideal for targeted drug delivery. Several studies using aptamers for targeted PDT have been reported in the literature.^{73–75} In the first study the aptamer AS1411, a 26-base guanine-rich oligonucleotide also known as anti-nucleolin aptamer, was conjugated to 13 nm AuNPs *via* Au-S bond.⁷³ The G-quadruplex conformation adopted by the aptamer allows its interaction with nucleolin but it also makes it possible for porphyrins to be intercalated within the structure. Therefore, the photosensitiser N-methylmesoporphyrin IX (NMM) was conjugated to form NMM-AS1411-AuNPs. The G-quadruplex structure has an enhancement effect of the fluorescence of NMM, which is further enhanced by interactions with the AuNPs. *In vitro* studies with HeLa cells, which overexpress nucleolin, confirmed the selective interaction between AS1411 and nucleolin, leading to an improved internalisation and thus efficient white light-mediated PDT.⁷³ That same AS1411 aptamer was used as the targeting ligand for combined PDT/PTT and chemotherapy.⁷⁴ Yi *et al.* synthesised DNA coated-AuNRs functionalised with doxorubicin and 5, 10, 15, 20-tetrakis(1-methylpyridinium-4-yl) porphyrin (TMPyP4) *via* the DNA assembly. Additionally, the AS1411 aptamer was hybridised with the DNA assembly, which had a complementary sequence. The use of AuNRs, together with TMPyP4 and doxorubicin opens the possibility for a combined PTT/PDT and chemotherapy treatment. NIR (808 nm) and white light can be used to trigger PTT and PDT, respectively. Additionally, irradiation of the AuNRs with 808 nm also induces the release of doxorubicin into the nucleus of the cells, leading to the chemotherapeutic effect. The use of combination therapies was reported to give the best results. More importantly, the presence of AS1411 led to a three-fold improvement in intracellular uptake by HeLa cells, which contributed to an enhanced cytotoxicity reaching *ca.* 92 % cell death in contrast to the *ca.* 51 % cell death seen with non-targeted AuNRs.⁷⁴

Another aptamer, TLS11a has been reported to specifically recognise hepatocellular carcinoma cells.⁷⁵ Zhang and co-workers created a targeting system based on the presence of an aptamer, but also taking advantage of the increased glutathione (GSH) activity inside tumour cells. GSH activity involves cleaving disulfide bonds. The authors functionalised AuNPs with a thiolated TLS11a aptamer, which was labelled with chlorin e6 and coordinated to a

Cu(II) complex, which allowed the functionalisation with the anti-tumour prodrug AQ4N (di-N-oxide of 1,4-bis[2-dimethylaminoethyl-amino]5,8-dihydro xanthracene-9,10-dione, also known as banoxantrone). Reduction of AQ4N in hypoxic conditions produces the toxic drug AQ4, with anti-tumour activity. The fluorescence of chlorin e6 was quenched in the presence of the AuNPs. However, upon internalisation by cancer cells, the fluorescence can be regained due to the cleaving of the thiol bond between the AuNPs and the TSL11a aptamer by the enhanced tumour GSH activity. As a result, the chlorin e6-TSL11a-Cu(II)-AQ4N complex is released. Furthermore, the acidic pH in the tumour tissues leads to the release of both Cu(II) and AQ4N. At this point, several processes can take place. The release of Cu(II) ions induces the aggregation of the AuNPs, which is advantageous for the treatment of the cancer cells *via* PTT. Furthermore, the release of chlorin e6 is key for the treatment of the cells *via* PDT. Upon 670 nm irradiation for PDT, the tumour tissue becomes hypoxic, which is a suitable environment for the reduction of AQ4N into the toxic drug AQ4. Therefore, following enhanced cell internalisation due to the TSL11a aptamer, a combination of PTT/PDT and chemotherapy takes place, making these AuNPs ideal for multimodal cancer treatment.⁷⁵ The research by Zhang *et al.* builds on a previous study in which the authors targeted the increased GSH activity in cancer cells without the presence of other external targeting ligands.⁷⁶ In their work, 40 nm AuNPs functionalised with a thiolated heparin conjugated to the photosensitiser pheophorbide A (PhA) were synthesised. Heparin was deliberately chosen due to its water solubility, biocompatibility and anti-tumour activity. Upon internalisation by cancer cells, the GSH activity cleaves the PhA-heparin from the AuNPs, allowing the PhA to regain its fluorescence properties and induce effective PDT cytotoxicity in A549 tumours both *in vitro* and *in vivo*.⁷⁶

Folic and hyaluronic acids

The folate receptor has become an important target for cancer therapies given its overexpression in tumours, including ovarian, breast and lung cancers amongst others, and its low expression in healthy tissue.⁷⁷ The use of folic acid has been widely reported for the specific targeting of folate, including studies with gold nanoparticle-mediated PDT.^{78–80} Gold quantum clusters, gold nanoclusters and gold nanorods are some of the gold structures used for folate-targeted PDT. Nair *et al.* synthesised gold quantum clusters covered with lipoic acid, to which folic acid and the photosensitiser PpIX were conjugated using EDC-NHS coupling.⁷⁸ The clusters accumulated in C6 glial tumours, which overexpress the folate receptor, *in vivo* only 3 h after injection. The enhanced accumulation due to the folate targeting was optimal for the combination of fluorescence imaging and PDT within the same system.⁷⁸ In a similar study, Zhang *et al.* conjugated a PEGylated folic acid to GSH-coated gold nanoclusters,

followed by entrapping chlorin e6 *via* hydrophobic interactions with the PEG and passive adsorption to the gold surface.⁷⁹ *In vitro* evaluation was performed in folate positive MGC-803 gastric cancer as well as folate negative GES-1 gastric epithelial cells. The results showed increased internalisation in the cancer cells as compared to the epithelial cells, thus confirming the specific interaction between folic acid and the folate receptor, which lead to enhanced PDT. *In vivo* studies further confirmed the potential of the folic acid conjugated gold nanoclusters since they were easily accumulated within the tumour tissue, only 10 minutes after injection, leading to effective inhibition of tumour growth.⁷⁹ Finally, in a separate study, CTAB coated AuNRs functionalised with a folic acid-containing block copolymer and thiolated chlorin e6, in the form of NH₂-SS-chlorin e6, were used for targeted PDT of breast cancer cells.⁸⁰ The use of a thiolated chlorin e6 allows its release from the AuNRs upon internalisation by the cancer cells, due to the enhanced GSH activity found in tumours. Upon release, chlorin e6 can be used for PDT, in combination with PTT therapy *via* the AuNRs. Internalisation of the folic acid targeted AuNRs was better for MCF-7 breast cancer cells than for A549 lung cancer cells, given that overexpression of the folate receptor is only seen in MCF-7 cells. The enhanced internalisation correlated with an improved therapeutic effect for both therapies, PDT at 670 nm and PTT and 880 nm. The combination of PDT with PTT, even though was found to be beneficial relative to single PTT therapy, only showed a moderate improvement from the treatment of the cells with PDT only, which was already efficient by itself.⁸⁰ The three studies here described confirm the selectivity of folic acid towards folate receptors and the potential of using this targeting ligand for enhanced cell kill in cancer therapy.

The glycoproteins CD44 are highly expressed in many tumours and are involved in metastasis and tumour progression.⁸¹ CD44 glycoproteins specifically bind hyaluronic acid thus making them an attractive receptor for targeted PDT. Tham *et al.* used hyaluronic acid for an enhanced PDT of HeLa cells, which overexpress CD44 on their surface. The authors prepared AuNRs encapsulated with a silica layer, to which a silica modified zinc phthalocyanine (ZnPc-Si) was attached. Hyaluronic acid was then conjugated electrostatically, creating a layer around the AuNRs. Confirmation of the targeting ability of hyaluronic acid was obtained by *in vitro* studies with CD44 positive HeLa cells and CD44 negative MCF-7 cells. Following a 24 h incubation period, a three-fold higher uptake of AuNRs was observed for HeLa cells, as confirmed by confocal microscopy, flow cytometry and inductively coupled plasma optical emission spectrometry (ICP-OES). Upon internalisation, irradiation of the cells with a 730 nm laser activated both PDT, *via* the ZnPc, and PTT, *via* the AuNRs. The combination treatment further confirmed the selective interaction between hyaluronic acid and CD44 since, while only 48 % of MCF-7 cells died, up to 79 % of HeLa cells were destroyed.⁸¹ This study shows the

advantages of using hyaluronic acid for the selective targeting of CD44-overexpressing tumorigenic cells.

Conclusions

The present paper has provided a state-of-the-art review of the most recent advances in gold nanoparticle-mediated photodynamic therapy of cancer. It is clear the combination of photosensitisers with gold nanoparticles is advantageous for PDT. Gold nanoparticles are biocompatible and have a low intrinsic toxicity, which makes them ideal candidates for biological applications. Additionally, their large surface area-to-volume ratio allows their functionalisation not only with photosensitisers but also with many other ligands. The use of certain polymers such as PEG can avoid protein adsorption and opsonisation *via* the RES, thus increasing the blood circulation, beneficial for the increased uptake of nanoparticles in the tumour tissue. More importantly, the combination of gold nanoparticles with targeting ligands, *i.e.*, actively targeted PDT, can further enhance the partial selectivity of the photosensitisers to a specific tumour.

Another important advantage for the use of gold nanoparticles and other gold nanostructures is the possibility to combine PDT with other anti-cancer therapies. Many gold structures, particularly gold nanorods, are ideal for PTT, based on the localised increase in temperature inside the tumour, which leads to its destruction. The additional functionalisation of AuNPs with a chemotherapeutic drug, such as doxorubicin, opens the possibility to treat cancers *via* chemotherapy. Many studies have reported that the combination of two or more of such therapies greatly increases the inhibition of tumour growth and destruction of cancer cells. The use of photosensitiser functionalised AuNPs is not restricted to therapeutics. Theranostics, by which diagnosis and therapy is performed using the same nanosystem, can be achieved by combining fluorescence imaging of the tumours with PDT and several examples have been described.

The investigation of AuNPs for PDT has seen a considerable increase since the first report in 2002. The versatility of AuNPs for functionalisation with both photosensitiser and targeting molecules coupled with combined therapeutic modalities ensures that gold nanoconjugates have an important future for enhanced cancer therapy.

References

- 1 P. García Calavia and D. A. Russell, in *Photodynamic medicine: From bench to clinic*, eds. H. Kostron and T. Hasan, The Royal Society of Chemistry, Croydon, 2016, pp. 113–135.
- 2 E. Boisselier and D. Astruc, Gold nanoparticles in nanomedicine: preparations, imaging, diagnostics, therapies and toxicity, *Chem. Soc. Rev.*, 2009, **38**, 1759–1782.
- 3 L. Dykman and N. Khlebtsov, Gold nanoparticles in biomedical applications: recent advances and perspectives, *Chem. Soc. Rev.*, 2012, **41**, 2256–2282.
- 4 A. Bucharskaya, G. Maslyakova, G. Terentyuk, A. Yakunin, Y. Avetisyan, O. Bibikova, E. Tuchina, B. Khlebtsov, N. Khlebtsov and V. Tuchin, Towards Effective Photothermal/Photodynamic Treatment Using Plasmonic Gold Nanoparticles, *Int. J. Mol. Sci.*, 2016, **17**, 1295.
- 5 D. C. Hone, P. I. Walker, R. Evans-Gowing, S. FitzGerald, A. Beeby, I. Chambrier, M. J. Cook and D. A. Russell, Generation of cytotoxic singlet oxygen via phthalocyanine-stabilized gold nanoparticles: A potential delivery vehicle for photodynamic therapy, *Langmuir*, 2002, **18**, 2985–2987.
- 6 M. E. Wieder, D. C. Hone, M. J. Cook, M. M. Handsley, J. Gavrilovic and D. A. Russell, Intracellular photodynamic therapy with photosensitizer-nanoparticle conjugates: cancer therapy using a ‘Trojan horse’, *Photochem. Photobiol. Sci.*, 2006, **5**, 727–734.
- 7 M. Camerin, M. Magaraggia, M. Soncin, G. Jori, M. Moreno, I. Chambrier, M. J. Cook and D. A. Russell, The in vivo efficacy of phthalocyanine-nanoparticle conjugates for the photodynamic therapy of amelanotic melanoma, *Eur. J. Cancer*, 2010, **46**, 1910–1918.
- 8 G. Obaid and D. A. Russell, in *Handbook of photomedicine*, eds. M. R. Hamblin and Y.-Y. Huang, Taylor & Francis, Boca Raton, 2013, pp. 367–378.
- 9 M. Camerin, M. Moreno, M. J. Marín, C. L. Schofield, I. Chambrier, M. J. Cook, O. Coppellotti, G. Jori and D. A. Russell, Delivery of a hydrophobic phthalocyanine photosensitizer using PEGylated gold nanoparticle conjugates for the in vivo photodynamic therapy of amelanotic melanoma, *Photochem. Photobiol. Sci.*, 2016, **15**, 618–625.
- 10 P. García Calavia, M. J. Marín, I. Chambrier, M. J. Cook and D. A. Russell, Towards optimisation of surface enhanced photodynamic therapy of breast cancer cells using gold nanoparticle-photosensitiser conjugates, *Photochem. Photobiol. Sci.*, 2018, **17**, 281–289.
- 11 X. Huang, X.-J. Tian, W.-L. Yang, B. Ehrenberg and J.-Y. Chen, The conjugates of gold nanorods and chlorin e6 for enhancing the fluorescence detection and photodynamic therapy of cancers, *Phys. Chem. Chem. Phys.*, 2013, **15**, 15727–15733.
- 12 Y. Zhang, K. Aslan, M. J. R. Previte and C. D. Geddes, Plasmonic engineering of singlet

- oxygen generation., *Proc. Natl. Acad. Sci. U.S.A.*, 2008, **105**, 1798–1802.
- 13 W. Deng, F. Xie, H. T. M. C. M. Baltar and E. M. Goldys, Metal-enhanced fluorescence in the life sciences: here, now and beyond, *Phys. Chem. Chem. Phys.*, 2013, **15**, 15695–15708.
 - 14 S. Wang, P. Huang, L. Nie, R. Xing, D. Liu, Z. Wang, J. Lin, S. Chen, G. Niu, G. Lu and X. Chen, Single continuous wave laser induced photodynamic/plasmonic photothermal therapy using photosensitizer-functionalized gold nanostars, *Adv. Mater.*, 2013, **25**, 3055–3061.
 - 15 S. Kolemen, T. Ozdemir, D. Lee, G. M. Kim, T. Karatas, J. Yoon and E. U. Akkaya, Remote-Controlled Release of Singlet Oxygen by the Plasmonic Heating of Endoperoxide-Modified Gold Nanorods: Towards a Paradigm Change in Photodynamic Therapy, *Angew. Chem., Int. Ed.*, 2016, **55**, 3606–3610.
 - 16 S. Clement, W. Chen, A. G. Anwer and E. M. Goldys, Verteporfin conjugated to gold nanoparticles for fluorescent cellular bioimaging and X-ray mediated photodynamic therapy, *Microchim. Acta*, 2017, **184**, 1765–1771.
 - 17 C. Zhang, X. Cheng, M. Chen, J. Sheng, J. Ren, Z. Jiang, J. Cai and Y. Hu, Fluorescence guided photothermal/photodynamic ablation of tumours using pH-responsive chlorin e6-conjugated gold nanorods, *Colloids Surf. B*, 2017, **160**, 345–354.
 - 18 N. F. Gamaleia, E. D. Shishko, G. A. Dolinsky, A. B. Shcherbakov, A. V. Usatenko and V. V. Kholin, Photodynamic activity of hematoporphyrin conjugates with gold nanoparticles: Experiments in vitro, *Exp. Oncol.*, 2010, **32**, 44–47.
 - 19 W. Li, H. Zhang, X. Guo, Z. Wang, F. Kong, L. Luo, Q. Li, C. Zhu, J. Yang, Y. Lou, Y. Du and J. You, Gold Nanospheres-Stabilized Indocyanine Green as a Synchronous Photodynamic–Photothermal Therapy Platform That Inhibits Tumor Growth and Metastasis, *ACS Appl. Mater. Interfaces*, 2017, **9**, 3354–3367.
 - 20 H. Eshghi, A. Sazgarnia, M. Rahimizadeh, N. Attaran, M. Bakavoli and S. Soudmand, Protoporphyrin IX-gold nanoparticle conjugates as an efficient photosensitizer in cervical cancer therapy, *Photodiagnosis Photodyn. Ther.*, 2013, **10**, 304–312.
 - 21 E. Haimov, H. Weitman, S. Polani, H. Schori, D. Zitoun and O. Shefi, *meso* - Tetrahydroxyphenylchlorin-Conjugated Gold Nanoparticles as a Tool To Improve Photodynamic Therapy, *ACS Appl. Mater. Interfaces*, 2018, **10**, 2319–2327.
 - 22 K. Záruba, J. Králová, P. Rezanka, P. Poucková, L. Veverková and V. Král, Modified porphyrin-brucine conjugated to gold nanoparticles and their application in photodynamic therapy., *Org. Biomol. Chem.*, 2010, **8**, 3202–3206.
 - 23 J. Ohyama, Y. Hitomi, Y. Higuchi, M. Shinagawa, H. Mukai, M. Kodera, K. Teramura, T. Shishido and T. Tanaka, One-phase synthesis of small gold nanoparticles coated by a horizontal porphyrin monolayer., *Chem. Commun.*, 2008, 6300–6302.
 - 24 M. Ashjari, S. Dehfuly, D. Fatehi, R. Shabani and M. Koruji, Efficient functionalization of gold nanoparticles using cysteine conjugated protoporphyrin IX for singlet oxygen

- production in vitro, *RSC Adv.*, 2015, **5**, 104621–104628.
- 25 L. Vieira, M. L. Castilho, I. Ferreira, J. Ferreira-Strixino, K. C. Hewitt and L. Raniero, Synthesis and characterization of gold nanostructured Chorin e6 for Photodynamic Therapy, *Photodiagnosis Photodyn. Ther.*, 2017, **18**, 6–11.
 - 26 K. Hari, A. Pichaimani and P. Kumpati, Acridine orange tethered chitosan reduced gold nanoparticles: a dual functional probe for combined photodynamic and photothermal therapy, *RSC Adv.*, 2013, **3**, 20471–20479.
 - 27 M. E. Alea-Reyes, M. Rodrigues, A. Serrà, M. Mora, M. L. Sagristá, A. González, S. Durán, M. Duch, J. A. Plaza, E. Vallés, D. A. Russell and L. Pérez-García, Nanostructured materials for photodynamic therapy: synthesis, characterization and in vitro activity, *RSC Adv.*, 2017, **7**, 16963–16976.
 - 28 M. E. Alea-Reyes, O. Penon, P. García Calavia, M. J. Marín, D. A. Russell and L. Pérez-García, Synthesis and in vitro phototoxicity of multifunctional Zn(II)meso-tetrakis(4-carboxyphenyl)porphyrin-coated gold nanoparticles assembled via axial coordination with imidazole ligands, *J. Colloid Interface Sci.*, 2018, **521**, 81–90.
 - 29 Y. Cheng, A. C. Samia, J. D. Meyers, I. Panagopoulos, B. Fei and C. Burda, Highly efficient drug delivery with gold nanoparticle vectors for in vivo photodynamic therapy of cancer, *J. Am. Chem. Soc.*, 2008, **130**, 10643–10647.
 - 30 Y. Cheng, A. C. Samia, J. Li, M. E. Kenney, A. Resnick and C. Burda, Delivery and Efficacy of a Cancer Drug as a Function of the Bond to the Gold Nanoparticle Surface, *Langmuir*, 2010, **26**, 2248–2255.
 - 31 Y. Cheng, J. D. Meyers, A. M. Broome, M. E. Kenney, J. P. Basilion and C. Burda, Deep penetration of a PDT drug into tumors by noncovalent drug-gold nanoparticle conjugates, *J. Am. Chem. Soc.*, 2011, **133**, 2583–2591.
 - 32 M. K. K. Oo, Y. Yang, Y. Hu, M. Gomez, H. Du and HongjunWang, Gold Nanoparticle-Enhanced and Size-Dependent Generation of Reactive Oxygen Species from, *ACS Nano*, 2012, **6**, 1939–1947.
 - 33 H. Xu, C. Liu, J. Mei, C. Yao, S. Wang, J. Wang, Z. Li and Z. Zhang, Effects of light irradiation upon photodynamic therapy based on 5-aminolevulinic acid-gold nanoparticle conjugates in K562 cells via singlet oxygen generation, *Int. J. Nanomedicine*, 2012, **7**, 5029–5038.
 - 34 Z. Mohammadi, A. Sazgarnia, O. Rajabi, S. Soudmand, H. Esmaily and H. R. Sadeghi, An in vitro study on the photosensitivity of 5-aminolevulinic acid conjugated gold nanoparticles, *Photodiagnosis Photodyn. Ther.*, 2013, **10**, 382–388.
 - 35 B. Jang, J. Park, C. Tung, I. Kim and Y. Choi, Gold Nanorod-Photosensitizer Complex for Near-Infrared Fluorescence Imaging and Photodynamic/Photothermal Therapy In Vivo, *ACS Nano*, 2011, **5**, 1086–1094.
 - 36 S. Bhana, R. O'Connor, J. Johnson, J. D. Ziebarth, L. Henderson and X. Huang, Photosensitizer-loaded gold nanorods for near infrared photodynamic and

- photothermal cancer therapy, *J. Colloid Interface Sci.*, 2016, **469**, 8–16.
- 37 M. E. Alea-Reyes, J. Soriano, I. Mora-Espí, M. Rodrigues, D. A. Russell, L. Barrios and L. Pérez-García, Amphiphilic gemini pyridinium-mediated incorporation of Zn(II)meso-tetrakis(4-carboxyphenyl)porphyrin into water-soluble gold nanoparticles for photodynamic therapy, *Colloids Surf. B*, 2017, **158**, 602–609.
 - 38 L. Casal-Dujat, M. Rodrigues, A. Yagüe, A. C. Calpena, D. B. Amabilino, J. González-Linares, M. Borràs and L. Pérez-García, Gemini Imidazolium Amphiphiles for the Synthesis, Stabilization, and Drug Delivery from Gold Nanoparticles, *Langmuir*, 2012, **28**, 2368–2381.
 - 39 M. E. Alea-Reyes, A. González, A. C. Calpena, D. Ramos-López, J. de Lapuente and L. Pérez-García, Gemini pyridinium amphiphiles for the synthesis and stabilization of gold nanoparticles for drug delivery, *J. Colloid Interface Sci.*, 2017, **502**, 172–183.
 - 40 A. M. Fales, H. Yuan and T. Vo-Dinh, Silica-coated gold nanostars for combined surface-enhanced Raman scattering (SERS) detection and singlet-oxygen generation: A potential nanoplatform for theranostics, *Langmuir*, 2011, **27**, 12186–12190.
 - 41 S. H. Seo, B. M. Kim, A. Joe, H. W. Han, X. Chen, Z. Cheng and E. S. Jang, NIR-light-induced surface-enhanced Raman scattering for detection and photothermal/photodynamic therapy of cancer cells using methylene blue-embedded gold nanorod@SiO₂ nanocomposites, *Biomaterials*, 2014, **35**, 3309–3318.
 - 42 P. Huang, J. Lin, S. Wang, Z. Zhou, Z. Li, Z. Wang, C. Zhang, X. Yue, G. Niu, M. Yang, D. Cui and X. Chen, Photosensitizer-conjugated silica-coated gold nanoclusters for fluorescence imaging-guided photodynamic therapy, *Biomaterials*, 2013, **34**, 4643–4654.
 - 43 L. Ricciardi, L. Sancey, G. Palermo, R. Termine, A. De Luca, E. I. Szerb, I. Aiello, M. Ghedini, G. Strangi and M. La Deda, Plasmon-mediated cancer phototherapy: the combined effect of thermal and photodynamic processes, *Nanoscale*, 2017, **9**, 19279–19289.
 - 44 Y. Hu, Y. Yang, H. Wang and H. Du, Synergistic Integration of Layer-by-Layer Assembly of Photosensitizer and Gold Nanorings for Enhanced Photodynamic Therapy in the Near Infrared, *ACS Nano*, 2015, **9**, 8744–8754.
 - 45 H. D. Cui, D. H. Hu, J. N. Zhang, G. H. Gao, C. F. Zheng, P. Gong, X. H. Xi, Z. H. Sheng and L. T. Cai, Theranostic gold cluster nanoassembly for simultaneous enhanced cancer imaging and photodynamic therapy, *Chinese Chem. Lett.*, 2017, **28**, 1391–1398.
 - 46 J. Yan, H. Sun, J. Li, W. Qi and H. Wang, A theranostic plaster combining photothermal therapy and photodynamic therapy based on chlorin e6/gold nanorods (Ce6/Au nrs) composite, *Colloids Surf. A*, 2018, **537**, 460–466.
 - 47 Z. Kautzka, S. Clement, E. M. Goldys and W. Deng, Light-triggered liposomal cargo delivery platform incorporating photosensitizers and gold nanoparticles for enhanced

- singlet oxygen generation and increased cytotoxicity, *Int. J. Nanomedicine*, 2017, **12**, 969–977.
- 48 M. Lee, H. Lee, N. Vijayakameswara Rao, H. S. Han, S. Jeon, J. Jeon, S. Lee, S. Kwon, Y. D. Suh and J. H. Park, Gold-stabilized carboxymethyl dextran nanoparticles for image-guided photodynamic therapy of cancer, *J. Mater. Chem. B*, 2017, **5**, 7319–7327.
 - 49 F. Ghorbani, N. Attaran-Kakhki and A. Sazgarnia, The synergistic effect of photodynamic therapy and photothermal therapy in the presence of gold-gold sulfide nanoshells conjugated Indocyanine green on HeLa cells, *Photodiagnosis Photodyn. Ther.*, 2017, **17**, 48–55.
 - 50 A. El-Hussein, I. Mfouo-Tynga, M. Abdel-Harith and H. Abrahamse, Comparative study between the photodynamic ability of gold and silver nanoparticles in mediating cell death in breast and lung cancer cell lines, *J. Photochem. Photobiol. B Biol.*, 2015, **153**, 67–75.
 - 51 G. Obaid, M. Broekgaarden, A. Bulin, H. Huang, J. Kuriakose and T. Hasan, Photonanomedicine : a convergence of photodynamic therapy and nanotechnology, *Nanoscale*, 2016, **8**, 12471–12503.
 - 52 N. Bertrand, J. Wu, X. Xu, N. Kamaly and O. C. Farokhzad, Cancer nanotechnology: The impact of passive and active targeting in the era of modern cancer biology, *Adv. Drug Deliv. Rev.*, 2014, **66**, 2–25.
 - 53 P. H. Liang, S. K. Wang and C. H. Wong, Quantitative analysis of carbohydrate-protein interactions using glycan microarrays: Determination of surface and solution dissociation constants, *J. Am. Chem. Soc.*, 2007, **129**, 11177–11184.
 - 54 G. Obaid, I. Chambrier, M. J. Cook and D. A. Russell, Cancer targeting with biomolecules: a comparative study of photodynamic therapy efficacy using antibody or lectin conjugated phthalocyanine-PEG gold nanoparticles, *Photochem. Photobiol. Sci.*, 2015, **14**, 737–47.
 - 55 T. Stuchinskaya, M. Moreno, M. J. Cook, D. R. Edwards and D. A. Russell, Targeted photodynamic therapy of breast cancer cells using antibody-phthalocyanine-gold nanoparticle conjugates, *Photochem. Photobiol. Sci.*, 2011, **10**, 822–831.
 - 56 O. Penon, M. J. Marín, D. A. Russell and L. Pérez-García, Water soluble, multifunctional antibody-porphyrin gold nanoparticles for targeted photodynamic therapy, *J. Colloid Interface Sci.*, 2017, **496**, 100–110.
 - 57 W. S. Kuo, C. N. Chang, Y. T. Chang, M. H. Yang, Y. H. Chien, S. J. Chen and C. S. Yeh, Gold Nanorods in Photodynamic Therapy, as Hyperthermia Agents, and in Near-Infrared Optical Imaging, *Angew. Chem., Int. Ed.*, 2010, **49**, 2711–2715.
 - 58 W. S. Kuo, Y. T. Chang, K. C. Cho, K. C. Chiu, C. H. Lien, C. S. Yeh and S. J. Chen, Gold nanomaterials conjugated with indocyanine green for dual-modality photodynamic and photothermal therapy, *Biomaterials*, 2012, **33**, 3270–3278.
 - 59 C. K. Chu, Y. C. Tu, J. H. Hsiao, J. H. Yu, C. K. Yu, S. Y. Chen, P. H. Tseng, S. Chen, Y. W.

- Kiang and C. C. Yang, Combination of photothermal and photodynamic inactivation of cancer cells through surface plasmon resonance of a gold nanoring., *Nanotechnology*, 2016, **27**, 115102.
- 60 Y. He, J. H. Hsiao, J. H. Yu, P. H. Tseng, W. H. Hua, M. C. Low, Y. H. Tsai, C. J. Cai, C. C. Hsieh, Y. W. Kiang, C. C. Yang and Z. Zhang, Cancer cell death pathways caused by photothermal and photodynamic effects through gold nanoring induced surface plasmon resonance, *Nanotechnology*, 2017, **28**, 275101.
 - 61 P. García Calavia, I. Chambrier, M. J. Cook, A. H. Haines, R. A. Field and D. A. Russell, Targeted photodynamic therapy of breast cancer cells using lactose-phthalocyanine functionalized gold nanoparticles Targeted photodynamic therapy of breast cancer cells using lactose- phthalocyanine functionalized gold nanoparticles, *J. Colloid Interface Sci.*, 2018, **512**, 249–259.
 - 62 G. Obaid, I. Chambrier, M. J. Cook and D. A. Russell, Targeting the oncofetal thomsen-friedenreich disaccharide using jacalin-PEG phthalocyanine gold nanoparticles for photodynamic cancer therapy, *Angew. Chem., Int. Ed.*, 2012, **51**, 6158–6162.
 - 63 Y. Cheng, J. D. Meyers, R. S. Agnes, T. L. Doane, M. E. Kenney, A. M. Broome, C. Burda and J. P. Basilion, Addressing brain tumors with targeted gold nanoparticles: A new gold standard for hydrophobic drug delivery?, *Small*, 2011, **7**, 2301–2306.
 - 64 J. D. Meyers, Y. Cheng, A. M. Broome, R. S. Agnes, M. D. Schluchter, S. Margevicius, X. Wang, M. E. Kenney, C. Burda and J. P. Basilion, Peptide-Targeted Gold Nanoparticles for Photodynamic Therapy of Brain Cancer, *Part. Part. Syst. Character.*, 2015, **32**, 448–457.
 - 65 S. Dixit, T. Novak, K. Miller, Y. Zhu, M. E. Kenney and A. M. Broome, Transferrin receptor-targeted theranostic gold nanoparticles for photosensitizer delivery in brain tumors, *Nanoscale*, 2015, **7**, 1782–1790.
 - 66 S. Dixit, K. Miller, Y. Zhu, E. McKinnon, T. Novak, M. E. Kenney and A. M. Broome, Dual Receptor-Targeted Theranostic Nanoparticles for Localized Delivery and Activation of Photodynamic Therapy Drug in Glioblastomas, *Mol. Pharm.*, 2015, **12**, 3250–3260.
 - 67 J. Yu, C. H. Hsu, C. C. Huang and P. Y. Chang, Development of therapeutic Au-methylene blue nanoparticles for targeted photodynamic therapy of cervical cancer cells, *ACS Appl. Mater. Interfaces*, 2015, **7**, 432–41.
 - 68 W. Li, X. Guo, F. Kong, H. Zhang, L. Luo, Q. Li, C. Zhu, J. Yang, Y. Du and J. You, Overcoming photodynamic resistance and tumor targeting dual-therapy mediated by indocyanine green conjugated gold nanospheres, *J. Control. Release*, 2017, **258**, 171–181.
 - 69 J. Wu, Y. Lin, H. Li, Q. Jin and J. Ji, Zwitterionic stealth peptide-capped 5-aminolevulinic acid prodrug nanoparticles for targeted photodynamic therapy, *J. Colloid Interface Sci.*, 2017, **485**, 251–259.
 - 70 J. Liu, H. Liang, M. Li, Z. Luo, J. Zhang, X. Guo and K. Cai, Tumor acidity activating

- multifunctional nanoplatform for NIR-mediated multiple enhanced photodynamic and photothermal tumor therapy, *Biomaterials*, 2018, **157**, 107–124.
- 71 F. Xia, W. Hou, C. Zhang, X. Zhi, J. Cheng, J. M. de la Fuente, J. Song and D. Cui, pH-responsive gold nanoclusters-based nanoprobe for lung cancer targeted near-infrared fluorescence imaging and chemo-photodynamic therapy, *Acta Biomater.*, 2018, **68**, 308–319.
 - 72 A. V Lakhin, V. Z. Tarantul and L. V Gening, Aptamers: problems, solutions and prospects, *Acta Naturae*, 2013, **5**, 34–43.
 - 73 J. Ai, Y. Xu, B. Lou, D. Li and E. Wang, Multifunctional AS1411-functionalized fluorescent gold nanoparticles for targeted cancer cell imaging and efficient photodynamic therapy, *Talanta*, 2014, **118**, 54–60.
 - 74 Y. Yi, H. Wang, X. Wang, Q. Liu, M. Ye and W. Tan, A Smart, Photocontrollable Drug Release Nanosystem for Multifunctional Synergistic Cancer Therapy, *ACS Appl. Mater. Interfaces*, 2017, **9**, 5847–5854.
 - 75 D. Zhang, A. Zheng, J. Li, M. Wu, L. Wu, Z. Wei, N. Liao, X. Zhang, Z. Cai, H. Yang, G. Liu, X. Liu and J. Liu, Smart Cu(II)-aptamer complexes based gold nanoplatform for tumor micro-environment triggered programmable intracellular prodrug release, photodynamic treatment and aggregation induced photothermal therapy of hepatocellular carcinoma, *Theranostics*, 2017, **7**, 164–179.
 - 76 L. Li, M. Nurunnabi, M. Nafiujjaman, Y. K. Lee and K. M. Huh, GSH-mediated photoactivity of pheophorbide a-conjugated heparin/gold nanoparticle for photodynamic therapy, *J. Control. Release*, 2013, **171**, 241–250.
 - 77 A. Cheung, H. J. Bax, D. H. Josephs, K. M. Ilieva, G. Pellizzari, J. Opzoomer, J. Bloomfield, M. Fittall, A. Grigoriadis, M. Figini, S. Canevari, J. F. Spicer, A. N. Tutt and S. N. Karagiannis, Targeting folate receptor alpha for cancer treatment, *Oncotarget*, 2016, **7**, 52553–52574.
 - 78 L. V. Nair, S. S. Nazeer, R. S. Jayasree and A. Ajayaghosh, Fluorescence Imaging Assisted Photodynamic Therapy Using Photosensitizer-Linked Gold Quantum Clusters, *ACS Nano*, 2015, **9**, 5825–5832.
 - 79 C. Zhang, C. Li, Y. Liu, J. Zhang, C. Bao, S. Liang, Q. Wang, Y. Yang, H. Fu, K. Wang and D. Cui, Gold nanoclusters-based nanoprobe for simultaneous fluorescence imaging and targeted photodynamic therapy with superior penetration and retention behavior in tumors, *Adv. Funct. Mater.*, 2015, **25**, 1314–1325.
 - 80 J. Choi, S.-E. Lee, J.-S. Park and S. Y. Kim, Gold nanorod-photosensitizer conjugates with glutathione-sensitive linkages for synergistic cancer photodynamic/photothermal therapy, *Biotechnol. Bioeng.*, 2018, **115**, 1340–1354.
 - 81 H. P. Tham, H. Chen, Y. H. Tan, Q. Qu, S. Sreejith, L. Zhao, S. S. Venkatraman and Y. Zhao, Photosensitizer Anchored Gold Nanorods for Targeted Combinational Photothermal and Photodynamic Therapy, *Chem. Commun.*, 2016, **52**, 8854–8857.